Identification of Keratinocyte Cytoprotectants against Toxicity by the Multikinase Inhibitor Sorafenib Using Drug Repositioning

Yayoi Kamata[1,2], Rui Kato[1,3], Mitsutoshi Tominaga[1,2], Sumika Toyama[1], Eriko Komiya[1], Jun Utsumi[1], Takahide Kaneko[3], Yasushi Suga[2,3] and Kenji Takamori[1,2,3]

Hand–foot skin reaction is the most common adverse event of multikinase inhibitors, such as sorafenib. Although hand–foot skin reaction is not life threatening, severe cases impair quality of life because of pain and reduced activities of daily living. However, the pathological mechanisms of hand–foot skin reaction have not yet been elucidated in detail, and there is currently no effective treatment. We aimed to identify keratinocyte cytoprotectants against sorafenib toxicity. The screening of cytoprotectants against sorafenib toxicity was performed using cultured normal human epidermal keratinocytes or a reconstructed human epidermis model and off-patent approved drugs in the Prestwick Chemical library. Among 1273 drugs in the chemical library, 8 dose-dependently increased cell viability by >200% in the presence of sorafenib. In the presence of sorafenib, the number of proliferating cell nuclear antigen–positive cells was significantly higher in clofazimine-, cyclosporin A–, and itraconazole-treated reconstructed human epidermis models than in sorafenib-treated models, and candidate drugs suppressed sorafenib-induced apoptosis in normal human epidermal keratinocytes. In addition, clofazimine, itraconazole, and pyrvinium pamoate significantly recovered the phosphorylation of extracellular signal–regulated kinase 1/2 in the presence of sorafenib. Collectively, hit drugs promoted cell viability and normalized keratinocyte proliferation in the presence of sorafenib. These candidate drugs have potential as treatments for multikinase inhibitor–induced hand–foot skin reaction.

Keywords: Apoptosis, Drug development, Hand-foot skin reaction, Keratinocyte, Multikinase inhibitor

JID Innovations (2024);**4:**100271 doi:10.1016/j.xjidi.2024.100271

INTRODUCTION

Oral multikinase inhibitors (MKI) (eg, sorafenib, sunitinib, regorafenib, lenvatinib, pazopanib, and vandetanib) reduce the activation of various Y kinases and ultimately suppress tumor growth and angiogenesis (Ancker et al, 2019; Cabanillas et al, 2019; Grandinetti and Goldspiel, 2007; Llovet et al, 2018). MKIs are associated with cutaneous toxicity, such as hand–foot skin reaction (HFSR), skin eruptions, and desquamation (Autier et al, 2008; Grothey et al, 2013; Lacouture et al, 2008; Lipworth et al, 2009; McLellan et al, 2015). Sorafenib is an MKI that is approved for the treatment of metastatic and unresectable renal cell carcinoma, hepatocellular carcinoma, and refractory differentiated thyroid cancer (Cabanillas et al, 2019; Carlomagno et al, 2006; Lipworth et al, 2009). It inhibits the protein kinase activity of C-RAF, B-RAF, VEGFR2 and 3, PDGFRβ, c-KIT, FLT3, and RET, which play important roles in tumor progression and angiogenesis (Adnane et al, 2006; Carlomagno et al, 2006; Grandinetti and Goldspiel, 2007). Phases II and III trials reported that the incidence of HFSR by sorafenib was 10–62%, and symptoms appeared within 2–6 weeks of treatment (Autier et al, 2008; Lacouture et al, 2008; Lipworth et al, 2009). Other MKIs, such as sunitinib, regorafenib, and lenvatinib, also caused HFSR as an adverse event in at least 50% of patients (Ancker et al, 2019; Krishnamoorthy et al, 2015; Lipworth et al, 2009).

A prodromal symptom of HFSR is characterized by initial dysesthesia, such as tingling, burning, and painful sensations, on the palms and soles (Autier et al, 2008; Lipworth et al, 2009). Typical symptoms of MKI-associated HFSR are tender blisters, cracks, and erythematous and edematous lesions, particularly in areas of friction or pressure, such as the palms and soles (Autier et al, 2008; Lacouture et al, 2008; Lipworth et al, 2009). Painful callus-like hyperkeratotic plaques are common in patients with MKI-induced HFSR (Autier et al, 2008). Because sorafenib targets the protein kinases involved in angiogenesis (eg, VEGFR, PDGFR, and c-KIT) and tumor growth signaling (eg, C-RAF and B-RAF), it may directly affect dermal blood vessels and epidermal basal cells. MKI-related HFSR of grade ≥2 has been identified as a

[1]*Juntendo Itch Research Center (JIRC), Institute for Environmental and Gender-Specific Medicine, Juntendo University Graduate School of Medicine, Chiba, Japan;* [2]*Anti-Aging Skin Research Laboratory, Juntendo University Graduate School of Medicine, Chiba, Japan; and* [3]*Department of Dermatology, Juntendo University Urayasu Hospital, Chiba, Japan*

Correspondence: Kenji Takamori, Juntendo Itch Research Center (JIRC), Institute for Environmental and Gender-Specific Medicine, Juntendo University Graduate School of Medicine, 2-1-1 Tomioka, Urayasu-shi, Chiba 279-0021, Japan. E-mail: ktakamor@juntendo.ac.jp

Abbreviations: ERK, extracellular signal–regulated kinase; EthD-III, ethidium homodimer III; HFSR, hand–foot skin reaction; K, keratin; MKI, multikinase inhibitor; NHEK, normal human epidermal keratinocyte; PBST, PBS containing 0.2% Tween 20; PCNA, proliferating cell nuclear antigen; RHE, reconstructed human epidermis

Received 22 December 2022; revised 4 December 2023; accepted 3 February 2024; accepted manuscript published online XXX; corrected proof published online XXX

Cite this article as: JID Innovations 2024;4:100271

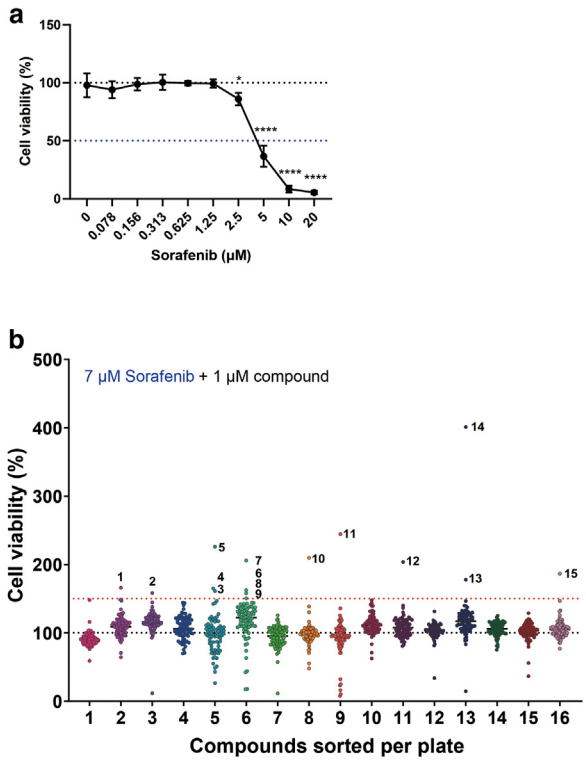

Figure 1. Screening of cytoprotectants against the cytotoxicity of sorafenib in NHEKs. (**a**) NHEKs were incubated at 37 °C overnight with each concentration of sorafenib before CCK-8 assay. Data were evaluated by a 1-way ANOVA followed by Dunnett's test; $^{****}P < .0001$ and $^{*}P < .05$. (**b**) NHEKs were incubated at 37 °C overnight with 7 μM sorafenib and 1 μM each off-patent approved drugs before the CCK-8 assay. The black dotted line represents 100% cell viability after a single treatment with 7 μM sorafenib. The red dotted line shows the threshold (150% cell viability) for positive hit drugs. All results are presented as the mean ± SD of triplicate wells in the single plate. CCK-8, Cell Counting Kit-8; NHEK, normal human epidermal keratinocyte.

clinical marker of the efficacy of MKI in patients (Kobayashi et al, 2019; Wang et al, 2019). Although HFSR is not life threatening, severe cases impair QOL because of pain, infection, and reduced activities of daily living and may lead to treatment discontinuation or dose reductions. The management of MKI-induced HFSR involves various palliative treatments, such as emollients; keratolytics (eg, 20–40% urea and 5–10% salicylic acid); corticosteroids; retinoids (eg, tazarotene);

Table 1. Cell Viability of 15 Hit Compounds in Primary Screening

Number	ID	Chemical Name	Therapeutic Effect	Cell Viability, %	*P*-Value[1]
1	02E02	Bromocriptine mesylate	Antiparkinsonian	166.0 ± 7.0	< .0001****
2	03E06	Tolfenamic acid	Analgesic	158.4 ± 7.8	.0002***
3	05B09	N6-methyladenosine	Antineoplastic	161.3 ± 32.2	.016*
4	05B10	Guanfacine hydrochloride	Antihypertensive	188.1 ± 46.5	.037*
5	05F07	Clofazimine	Antibacterial	171.3 ± 2.4	< .0001****
6	06C06	Chicago sky blue 6B	—	162.6 ± 13.2	.001**
7	06D06	Cyclosporin A	Immunosuppressant	205.9 ± 30.1	.004**
8	06F04	Calcipotriene	Antipsoriatic	174.5 ± 38.7	.038*
9	06F08	Meclozine dihydrochloride	Antiemetic	150.6 ± 18.1	.008**
10	08A08	Itraconazole	Antifungal	209.8 ± 20.5	.001***
11	09B11	Avermectin B1a	Antihelmintic	244.4 ± 12.4	< .0001****
12	11G11	Luteolin	Expectorant	203.7 ± 28.4	.003**
13	13H02	Halofantrine hydrochloride	Antimalarial	177.8 ± 11.5	.0003***
14	13H11	Pyrvinium pamoate	Antihelmintic	401.1 ± 97.3	.006**
15	16B08	Tolcapone	Antiparkinsonian	186.6 ± 25.3	.004**

Abbreviation: ID, identification.
All results are presented as the mean ± SD of triplicate wells in the single plate. $^{*}P < .05$, $^{**}P < .01$, $^{***}P < .001$, and $^{****}P < .0001$.
[1]Student's *t*-test (vs vehicle with 7 μM sorafenib).

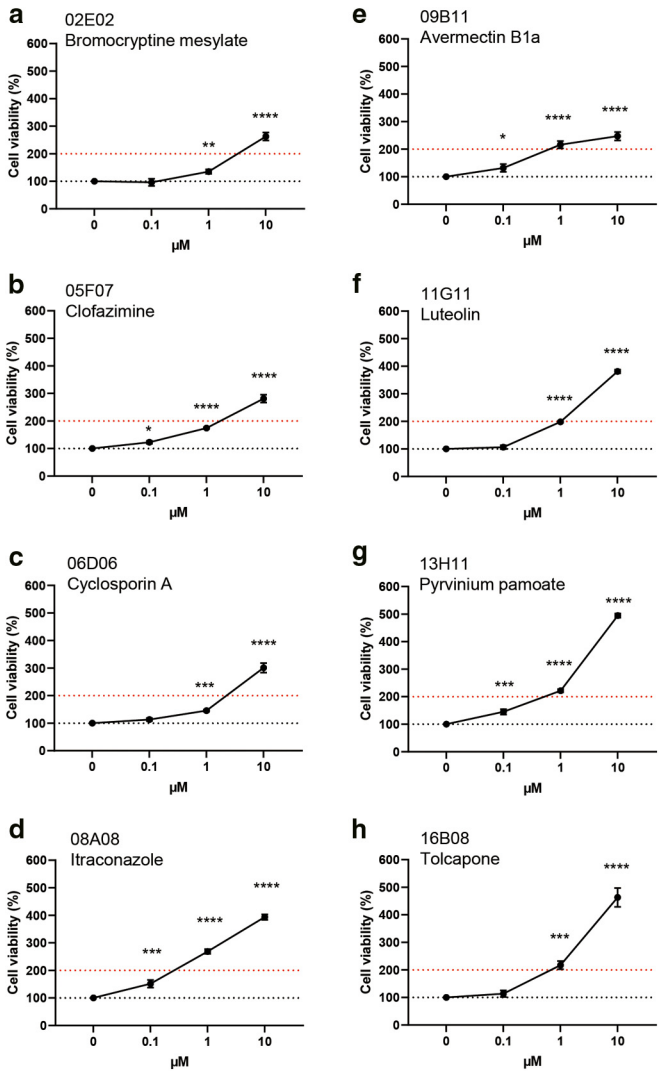

Figure 2. Hit drugs dose-dependently promote cell viability in the presence of sorafenib. NHEKs were incubated at 37 °C overnight with (**a**–**h**) each hit drug in the presence of 7 μM sorafenib. Cell viability was assessed by the CCK-8 assay. The black dotted line represents 100% cell viability after a single treatment with 7 μM sorafenib. The red dotted line shows the threshold (200% cell viability) for positive hit drugs. (**a**–**h**) Each graph is indicated with a plate location number. Data were evaluated by a 1-way ANOVA followed by Dunnett's test; $^{****}P < .0001$, $^{***}P < .001$, $^{**}P < .01$, and $^{*}P < .05$. All results are presented as the mean ± SD of triplicate wells in the single plate. CCK-8, Cell Counting Kit-8.

nonsteroidal anti-inflammatory drugs (eg, celecoxib); and the avoidance of mechanical stimuli, including hot water, detergents, and tight shoes and socks (Autier et al, 2008; Cabanillas et al, 2019; Lacouture et al, 2008; McLellan et al, 2015; Stanculeanu et al, 2017). However, the pathological mechanisms of HFSR remain unclear, and there is currently no treatment other than palliative therapy. Therefore, the development of effective therapy for MKI-induced HFSR is awaited.

In this study, we screened 1273 off-patent and approved drugs in the Prestwick Chemical Library and identified several cytoprotectants against sorafenib-induced keratinocyte toxicity using normal human epidermal keratinocytes (NHEKs) and a reconstructed human epidermis (RHE) model.

RESULTS

Identification of cytoprotectants against sorafenib cytotoxicity

Sorafenib dose-dependently decreased the viability of NHEKs (50% cell toxicity dose, 4.2 μM) (Figure 1a). We used 7 μM sorafenib (inhibition rate, 72.5%) to screen cytoprotectants. We then screened the Prestwick Chemical Library consisting of 1273 approved drugs at a final concentration of 1 μM in the presence of 7 μM sorafenib. Cell viability indicated the relative value to sorafenib only. Among 1273 drugs from the Prestwick Chemical Library, 15 increased cell viability by >150% in the presence of sorafenib (Figure 1b and Table 1).

Eight of these compounds—bromocriptine mesylate, avermectin B1a, clofazimine, cyclosporin A, itraconazole, luteolin, pyrvinium pamoate, and tolcapone—dose-dependently increased cell viability by >200% in the presence of sorafenib (Figure 2a–h). The effects of other hit drugs, including tolfenamic acid, N6-methyladenosine, guanfacine hydrochloride, Chicago sky blue 6B, calcipotriene, meclozine dihydrochloride, and halofantrine hydrochloride, were weaker than those of the 8 drugs (Figure 3). The cytotoxicity of these hit drugs was negligible at a final concentration of 1 μM in the absence of sorafenib but was significant at 10 μM (Figure 4a–o).

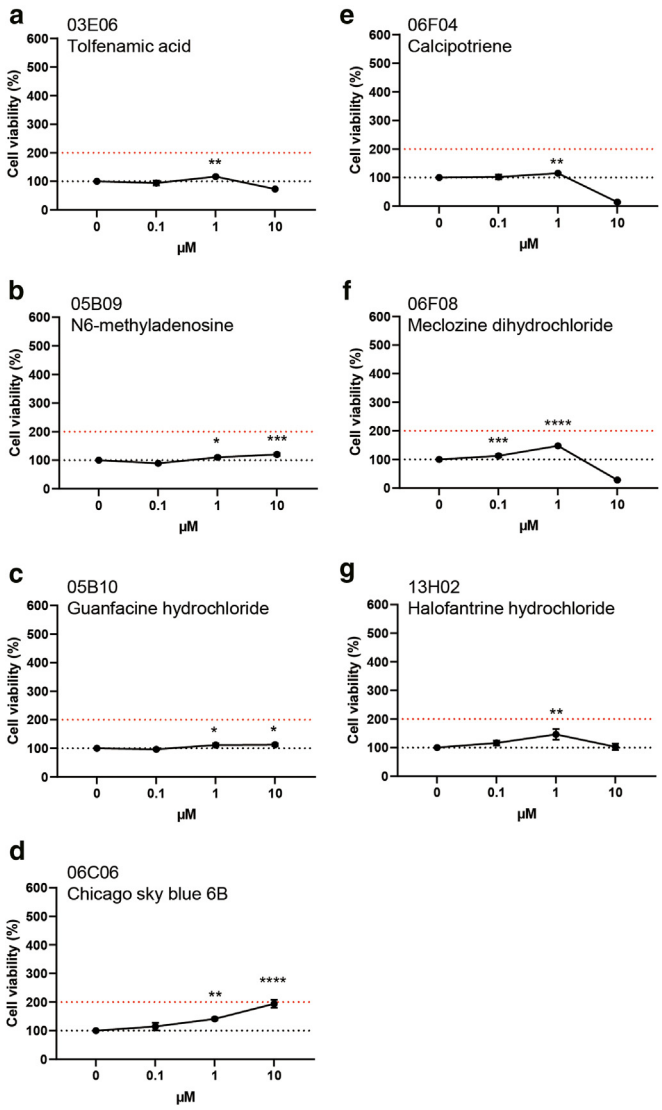

Figure 3. Second screening of hit drugs against sorafenib toxicity in NHEKs. NHEKs were incubated at 37 °C overnight with (**a**–**g**) each hit drug in the presence of 7 μM sorafenib. Cell viability was assessed by CCK-8 assay. The black dotted line represents 100% cell viability with a single treatment of 7 μM sorafenib. The red dotted line shows the threshold (200% cell viability) for positive hit drugs. Data were evaluated by a 1-way ANOVA followed by Dunnett's test; $^{****}P < .0001$, $^{***}P < .001$, $^{**}P < .01$, and $^{*}P < .05$. All results are presented as the means ± SD of triplicate wells in the single plate. CCK-8, Cell Counting Kit-8; NHEK, normal human epidermal keratinocyte.

Cytotoxicity of sorafenib in the RHE model

We histopathologically analyzed the cytotoxicity of sorafenib using the RHE model. Sorafenib was added to the medium in the RHE model and incubated for 96 hours before the collection of epidermal sheets (Figure 5a and b). Sorafenib dose-dependently decreased the cell viability of RHE (50% cell toxicity dose, 37.3 μM) (Figure 5c). Therefore, we used 40 μM sorafenib (inhibition rate, 59.1%) in experiments using the RHE model. Our preliminary study identified 4 candidate drugs—clofazimine (cell viability, mean ± SD: 76.7 ± 7.4%, $^{****}P < .0001$), cyclosporin A (55.1 ± 11.5%, $^{****}P < .0001$), itraconazole (73.6 ± 10.0%, $^{****}P < .0001$), and pyrvinium pamoate (65.6 ± 4.1%, $^{****}P < .0001$)—which significantly promoted keratinocyte viability compared with vehicle (29.7 ± 18.0%) in the sorafenib-treated RHE model (Figure 6). Other hit drugs, including bromocriptine mesylate, avermectin B1a, luteolin, and tolcapone, did not enhance cell viability (Figure 6). The histopathological study of the RHE model showed the cytoplasmic and nuclear vacuolation of basal and suprabasal keratinocytes in the sorafenib-treated group (Figure 5d and e). The number of vacuoles was higher in the sorafenib-treated group (area of vacuoles, mean ± SD: 398.1 ± 253.1 μm^2, $^{***}P = .0002$) than in the vehicle-treated group (88.0 ± 76.2 μm^2) (Figure 5f).

Influence of sorafenib and hit drugs on keratinocyte proliferation and differentiation

Immunohistochemistry was performed to establish whether the expression of proliferating cell nuclear antigen (PCNA) is a marker of cell proliferation. Sorafenib and/or hit drugs were

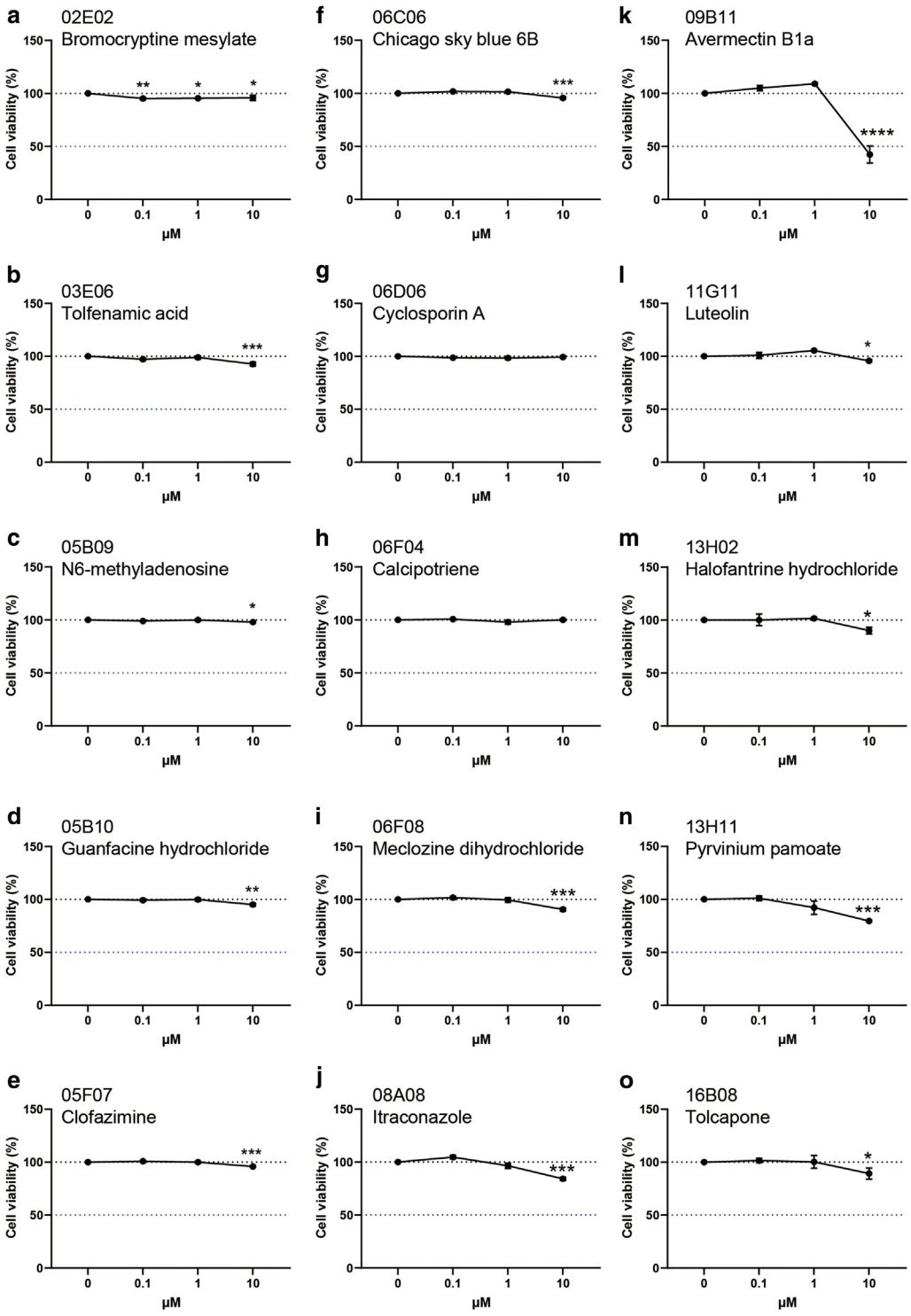

Figure 4. Cell toxicity of hit drugs towards NHEKs in the absence of sorafenib. NHEKs incubated at 37 °C overnight with (**a**–**o**) each hit drug in the absence of sorafenib. Cell viability was assessed by the CCK-8 assay. The black dotted line is the cell viability of the vehicle represented as 100%. Data were evaluated by a 1-way ANOVA followed by Dunnett's test; $^{****}P <$ .0001, $^{***}P <$ .001, $^{**}P <$ .01, and $^{*}P <$ .05. All results are presented as the means ± SD of triplicate wells in the single plate. CCK-8, Cell Counting Kit-8; NHEK, normal human epidermal keratinocyte.

added to the medium in the RHE model and incubated for 96 hours, and epidermal sheets were then collected (Figure 7a and b). The number of PCNA-positive keratinocytes was significantly lower in the sorafenib-treated group (PCNA-positive cells, mean ± SD: 56.1 ± 11.2%, $^{****}P <$ .0001) than in the vehicle-treated group (80.9 ± 7.1%) (Figure 7c and d). In the presence of sorafenib, PCNA-positive cells significantly increased after the addition of clofazimine (82.2 ± 8.3%, $^{****}P <$ .0001), cyclosporin A (75.6 ± 9.6%, $^{****}P <$ .0001), or itraconazole (83.9 ± 7.5%, $^{****}P <$ .0001) (Figure 7e–g and j). Pyrvinium pamoate did not restore PCNA expression (51.5 ± 10.8%, not significant) in the presence of sorafenib (Figure 7h). The negative control (without the primary antibody) is shown in Figure 7i. In the absence of sorafenib, PCNA expression was

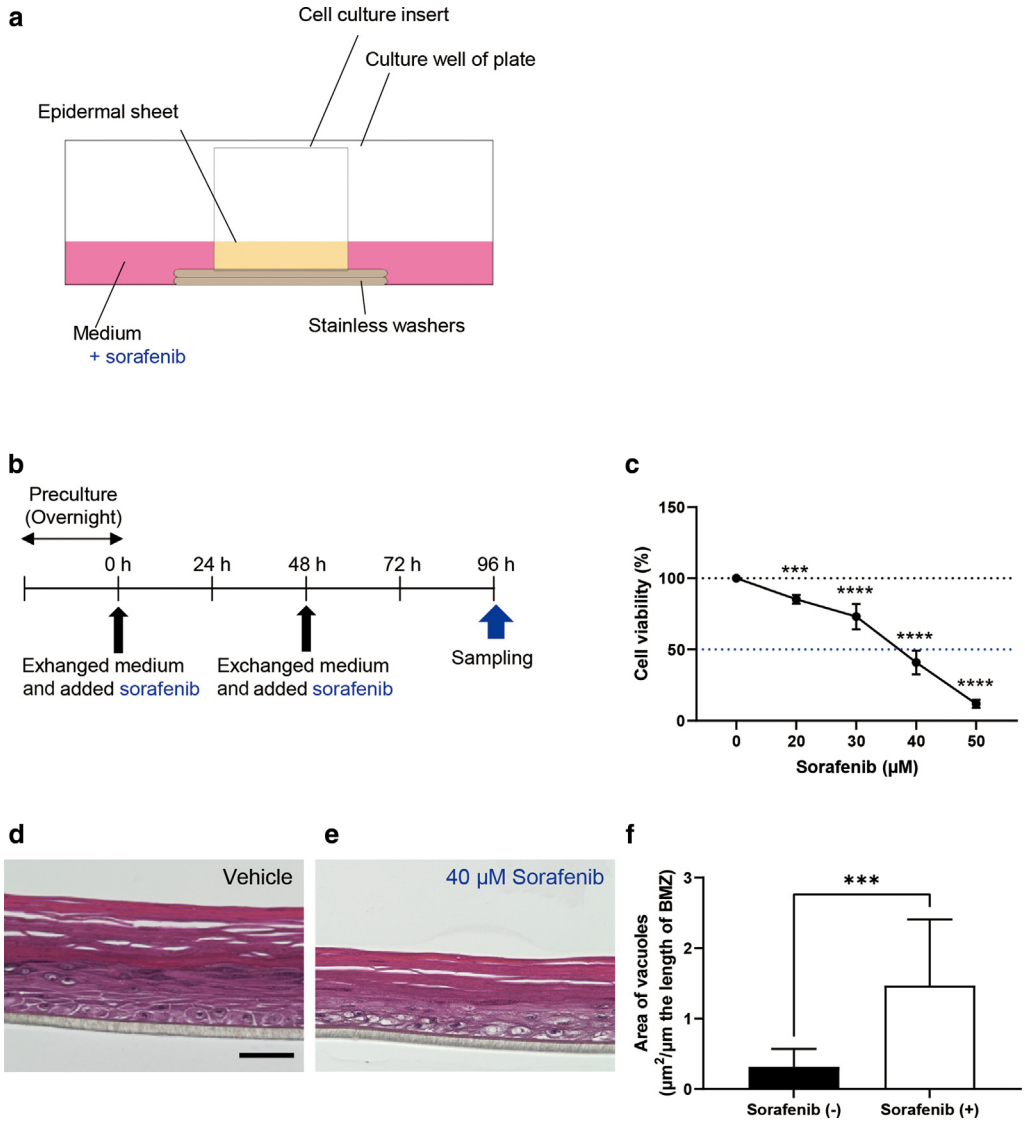

Figure 5. Cytotoxicity of sorafenib in the RHE model. (**a**) Schematic illustration of the RHE model. (**b**) Experimental schedule for the cytotoxic test. (**c**) Dose-dependent cytotoxicity of sorafenib toward the RHE model. Data were evaluated by a 1-way ANOVA followed by Dunnett's test; $^{****}P < .0001$ and $^{***}P < .001$. (**d**–**f**) H&E staining of the RHE model. RHE was incubated for 96 h with medium containing (**e**) 40 μM sorafenib or (**d**) DMSO (vehicle). Bar = 50 μm. (**f**) Areas of vacuolation were measured using an analysis application of the BZ-X800 series. Area of vacuoles were indicated as μm^2 per μm of the length of basement membrane zone and evaluated by the Student's *t*-test; $^{***}P = .0002$. The results were presented as the mean ± SD of triplicate epidermis in the same experiment. h, hour; RHE, reconstructed human epidermis.

similar in cells treated with clofazimine, cyclosporin A, or itraconazole and the vehicle, whereas pyrvinium pamoate reduced the number of PCNA-positive keratinocytes (Figure 8a–f).

We examined the expression of keratin (K)10 and K14 as differentiation and proliferation markers of keratinocytes, respectively. In the vehicle-treated group, K14 was detected at the stratum basale, and K10 was detected at the stratum spinosum (Figure 9a). K10 expression was significantly reduced (fluorescence intensity, mean ± SD: 4234 ± 2037 μm^2, $^{***}P < .001$), whereas K14 expression was slightly decreased (2481 ± 2416 μm^2, not significant) after the sorafenib treatment compared with that of vehicle (K10: 9445 ± 4090 μm^2 and K14: 3658 ± 2416 μm^2) (Figure 9b, g, and h). Their expression was markedly increased by clofazimine (K10: 9586 ± 3077 μm^2, $^{**}P < .01$ and K14: 6004 ± 3465 μm^2, $^{**}P < .01$) and cyclosporin A (K10: 15523 ± 3856 μm^2, $^{****}P < .0001$ and K14: 7420 ± 2260 μm^2, $^{***}P < .001$) compared with that of the vehicle in the presence of sorafenib (Figure 9c, d, g, and h). The K10-positive stratum spinosum was thinner in the sorafenib-treated group than in the vehicle-treated group (Figure 9a and b). However, clofazimine or cyclosporine A normalized the thickness of the K10-positive stratum spinosum more than sorafenib (Figure 9c and d). In the absence of sorafenib, clofazimine, cyclosporin A, and itraconazole did not affect K10 or K14 expression (Figure 10a–e). Pyrvinium pamoate significantly decreased K10 expression (1615 ± 2659 μm^2, $^{**}P < .01$) and slightly reduced K14 expression (1337 ± 2710 μm^2, not significant) in the absence of sorafenib (K10: 9445 ± 4090 μm^2 and K14: 3658 ± 2416 μm^2) (Figure 10f–h). In the presence of sorafenib, pyrvinium pamoate did not change K10 or K14 expression from that in the sorafenib-treated group (Figure 9f–h). In addition, we checked other epidermal differentiation markers, such as loricrin, involucrin, and FLG. Loricrin was expressed at stratum granulosum

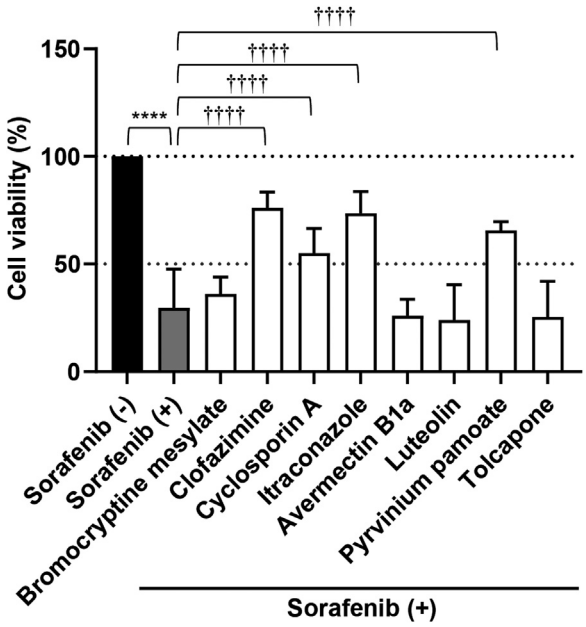

Figure 6. Preliminary screening of hit drugs against sorafenib toxicity in the RHE model. RHE was incubated for 96 h in the presence of 40 μM sorafenib and/or 10 μM of the candidate drug. Cell viability was analyzed by the MTT assay. Data were evaluated by a 1-way ANOVA followed by Tukey's multiple comparison test; $^{****}P < .0001$ (vs vehicle without sorafenib, black bar) and $^{††††}P < .0001$ (vs vehicle with sorafenib, gray bar). The results are presented as the means ± SD of triplicate epidermis in the same experiment. h, hour; RHE, reconstructed human epidermis.

in vehicle-treated group, whereas its expression was suppressed by sorafenib (Figure 11a and b). In the presence of sorafenib, loricrin expression was not restored by any hit drugs (Figure 11c–f and h). Involucrin was expressed at stratum spinosum and stratum granulosum (Figure12a), and FLG was expressed at stratum corneum and stratum granulosum in vehicle-treated group (Figure 13a). After treatment by sorafenib and candidate drug, involucrin and FLG expressions did not change compared with those of sorafenib-treated group (Figures 12b–f and h and 13b–f and h). The negative control (without primary antibody) is shown in Figures 11g, 12g, and 13g.

Analysis of the sorafenib-induced cell death mechanism

Next, we investigated the cell toxic mechanisms of sorafenib on keratinocytes. Annexin V–positive apoptotic cells were significantly increased in sorafenib-treated group compared with that in vehicle-treated group (Figure 14a and b). Almost all annexin V–positive cells costained with ethidium homodimer III (EthD-III), which was indicated at the late stage of apoptosis (Figure 14b, f, and g). In the presence of sorafenib, annexin V–positive apoptotic cells were decreased by adding clofazimine, cyclosporin A, or itraconazole compared with that in sorafenib-treated group (Figure 14c and d–f). Our preliminary result revealed that pyrvinium pamoate indicates autofluorescence using filters of GFP (excitation wavelength: 470 nm, emission wavelength: 525 nm) and Texas Red (excitation wavelength: 560 nm, emission wavelength: 630 nm) in fluorescence microscope (Figure 15e). Therefore, we did not use FITC-conjugated annexin V conjugate and EthD-III for analysis of pyrvinium pamoate; rather it was substituted by Alexa Fluor 647–conjugated annexin V. Pyrvinium pamoate did not indicate autofluorescence using a filter Cy5 (excitation wavelength: 640 nm, emission wavelength: 690 nm) for Alexa Fluor 647 (Figure 16e). On the other hand, autofluorescence was not observed in the other drugs or sorafenib-treated group (Figures 15a–d and 16a–d). In the presence of sorafenib, pyrvinium pamoate reduced the number of annexin V–positive cells compared with that in sorafenib-treated group (Figure 17a–d). In the absence of sorafenib, itraconazole was slightly increased in apoptotic cells, whereas other drugs did not show significant changes (Figures 18a–f and 19a–c).

Elucidation of cytoprotection mechanism by candidate compounds

Sorafenib inhibit c-Raf, upstream of MAPK/extracellular signal–regulated kinase (ERK) kinase/ERK1/2 pathway (Adnane et al, 2006). This pathway participates in various events, such as cell survival, cell proliferation, cell differentiation, and cell migration (Lavoie et al, 2020). Therefore, we examined changes in phosphorylation of ERK1/2 after incubation with sorafenib and/or hit drugs. Sorafenib suppressed ERK1/2 phosphorylation (Figure 20a), whereas coexistence of clofazimine, itraconazole, and pyrvinium pamoate significantly promoted the phosphorylation. In particular, clofazimine and pyrvinium pamoate strongly rescued ERK1/2 phosphorylation in the presence of sorafenib (Figure 20a and b). In the absence of sorafenib, each hit drugs significantly promoted ERK1/2 phosphorylation (Figure 20a and c).

DISCUSSION

Drug repositioning is a drug discovery strategy that explores alternative uses for off-patent approved drugs or failed developing compounds. In this study, we searched for

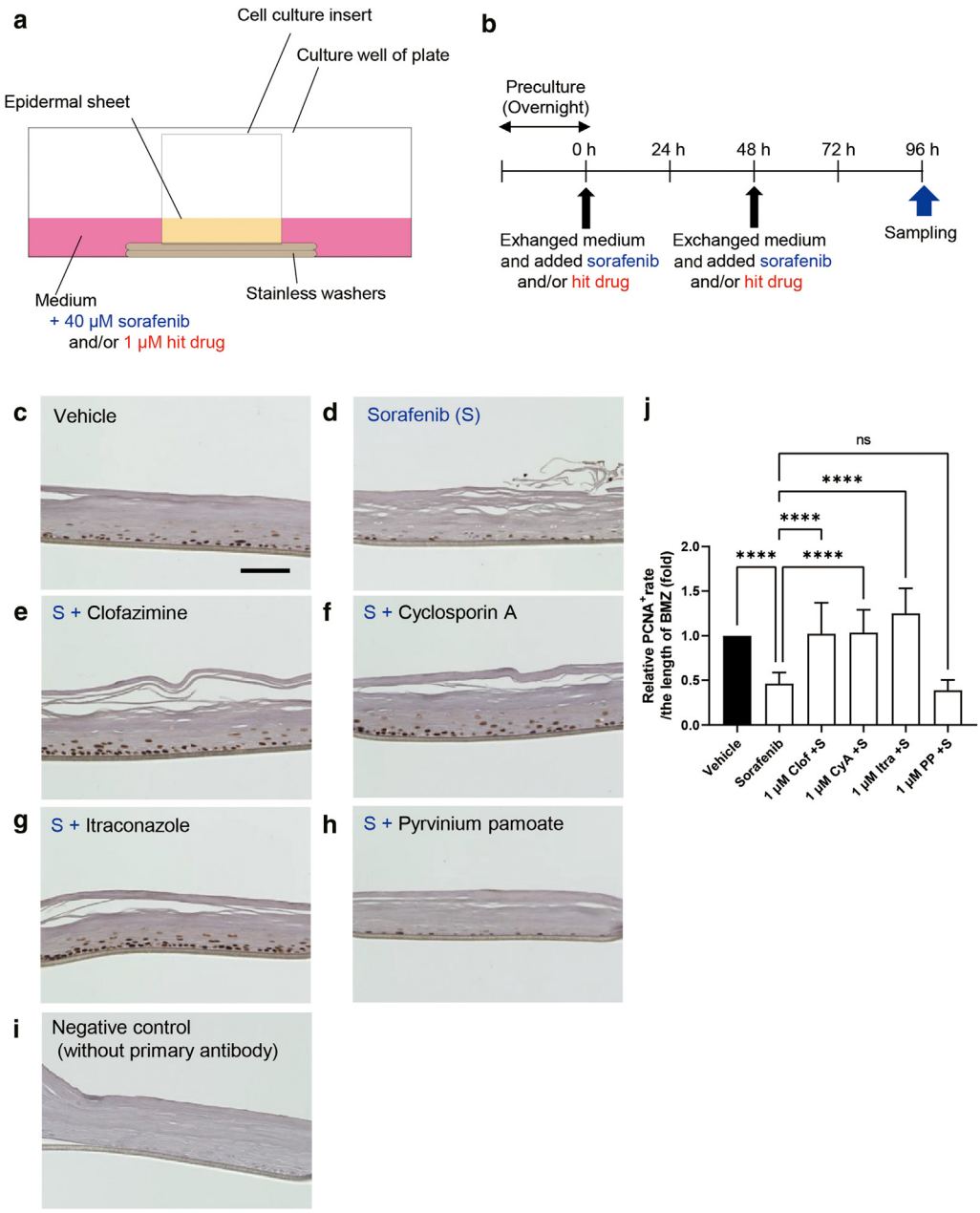

Figure 7. Detection of PCNA-positive cells in the sorafenib- and/or hit drug–treated RHE model. (**a**) Schematic illustration of the RHE model. (**b**) Experimental schedule for the screening of hit drugs. (**c–i**) Immunohistochemical staining of PCNA in the RHE model. Bar = 100 μm. (**j**) Quantification of PCNA-positive nuclei in all nuclei. PCNA-positive nuclei were manually counted and indicated as a relative value (%) of all nuclei. Relative PCNA-positive rate were indicated by the number of $PCNA^+$ cells per μm of the length of basement membrane zone. The results are presented as the mean ± SD of triplicate epidermis in the same experiment. Data were evaluated by a 1-way ANOVA followed by Tukey's test; $^{****}P <$ .0001. S denotes sorafenib, Clof denotes clofazimine, CyA denotes cyclosporin A, Itra denotes itraconazole, and PP denotes pyrvinium pamoate. h, hour; PCNA, proliferating cell nuclear antigen; RHE, reconstructed human epidermis.

keratinocyte cytoprotectants against sorafenib toxicity by screening the Prestwick Chemical Library, consisting of 1273 compounds. We identified clofazimine, cyclosporine A, itraconazole, and pyrvinium pamoate as cytoprotectants in NHEKs and the RHE model.

Candidate drug 1: clofazimine

Clofazimine is a lipophilic riminophenazine antibiotic that is used to treat mycobacterium infections, such as leprosy (Arbiser and Moschella, 1995; Cholo et al, 2012). By oxidizing the reduced form of clofazimine, ROS with antibiotic activity are produced (Arbiser and Moschella, 1995). It also interacts with the phospholipids of membranes, resulting in the generation of antimicrobial lysophospholipids, which promote bacterial membrane destabilization (Cholo et al, 2012). However, the keratinocyte proliferative and cytoprotective effects of clofazimine against sorafenib toxicity have yet to be reported. The adverse effect, the orange–pink or reddish–brown discoloration of the skin and the conjunctiva, has been reported (Arbiser and Moschella, 1995; Cholo et al, 2012).

Candidate drug 2: cyclosporin A

Cyclosporin A is an immunosuppressant agent isolated from *Tolypocladium inflatum* at Sandoz Laboratories in Basel (Switzerland) (Azzi et al, 2013). In the cytosol, cyclosporin A binds to cyclophilin and inhibits calcineurin, which exhibits serine/threonine phosphatase activity. Inactivated calcineurin fails to activate nuclear factor of activated T cells, and thus, T cells do not produce IL-2, which is involved in the activation

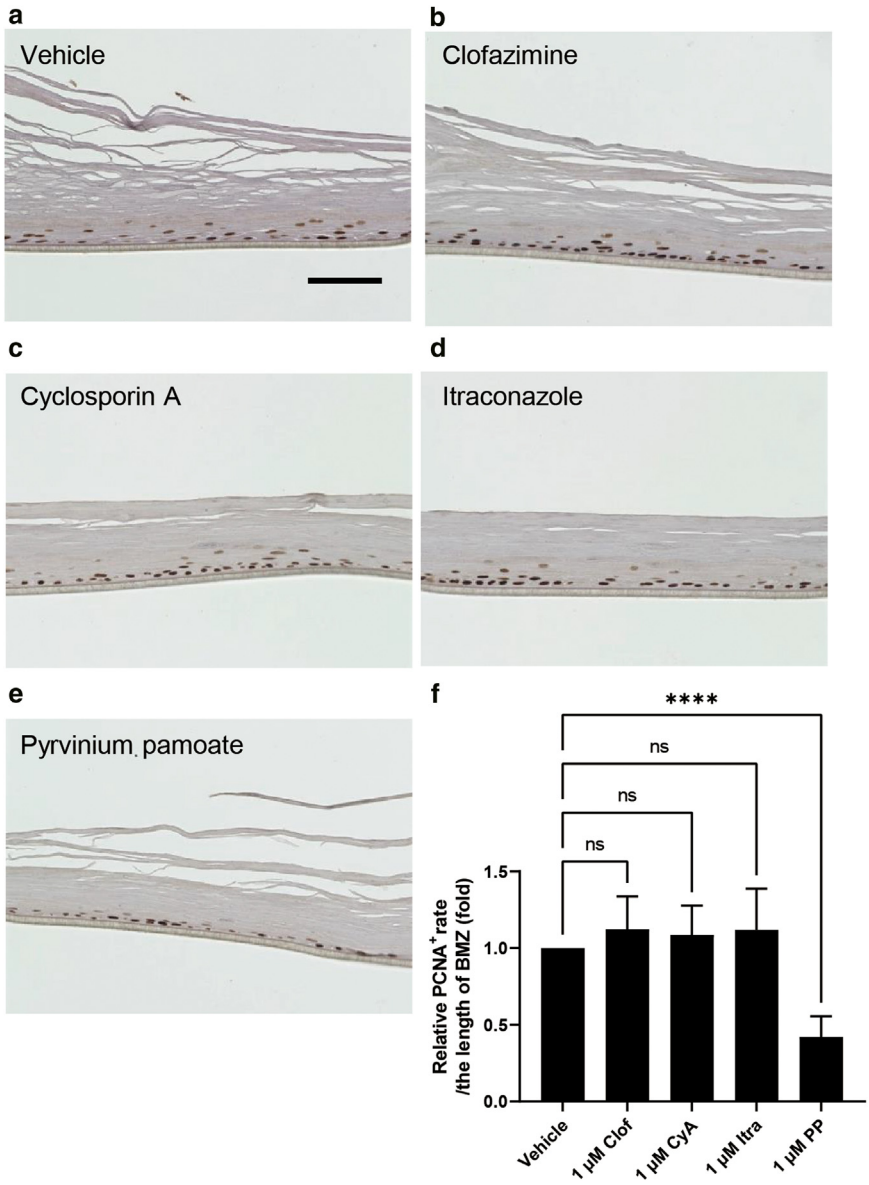

Figure 8. Detection of PCNA-positive cells in the hit drug–treated RHE model without sorafenib. (**a**–**e**) Immunohistochemical staining of PCNA in paraffin-embedded sections of the hit drug–treated RHE model. Bar = 100 μm. (**f**) Quantification of PCNA-positive nuclei among all nuclei. PCNA-positive nuclei were manually counted and indicated as a relative value (%) in all nuclei per μm of the length of the basement membrane zone. The results are presented as the means ± SD of triplicate epidermis in the same experiment. Data were evaluated by a 1-way ANOVA followed by Dunnett's multiple comparison test; $^{****}P <$ .0001. S denotes sorafenib, Clof denotes clofazimine, CyA denotes cyclosporin A, Itra denotes itraconazole, BMZ denotes basement membrane zone; and PP denotes pyrvinium pamoate. ns, not significant; PCNA, proliferating cell nuclear antigen; RHE, reconstructed human epidermis.

and proliferation of T cells (Amor et al, 2010; Azzi et al 2013). Cyclosporin A is known to induce renal dysfunction and hypertension as adverse effects (Ryan et al, 2010). In addition, it is possible to increase malignancy risk because of potent immunosuppression effects (Ryan et al, 2010). Therefore, it may be difficult to use for treatment of MKI-induced HFS in patients with cancer.

Candidate drug 3: itraconazole

Itraconazole is an azole antifungal drug that inhibits the ergosterol biosynthesis of fungal cell membranes by suppressing cytochrome P450 (Ahmadi et al, 2022; Saag and Dismukes, 1988). There were many strong cytochrome 3A4 inhibitors in the Prestwick Chemical Library, including azole antifungal drugs (eg, itraconazole, ketoconazole, and voriconazole), antiviral drugs (eg, indinavir and ritonavir), and clarithromycin. However, antiviral drugs and clarithromycin did not markedly affect the viability of sorafenib-treated NHEKs (Table 2). Therefore, cytochrome 3A4 inhibitory effects may not play a role in cytoprotectant effects against sorafenib. Azole antifungal drugs exhibit various biological activities without antifungal effects, such as anticancer effects, the inhibition of Gram-positive bacteria growth, and the induction of β-defencin 3 in human keratinocytes (Kanda et al, 2011; Sugita et al, 2010; Tsubamoto et al, 2017). The anticancer mechanisms of itraconazole involve the inhibition of Hedgehog signaling, protein kinase B/mechanistic target of rapamycin, Wnt-β-catenin signaling, and VEGF2 (Tsai and Tsai, 2019; Tsubamoto et al, 2017). Furthermore, itraconazole exerts anti-inflammatory effects and is effective against palmoplantar pustulosis (Mihara et al, 1998; Tsai and Tsai, 2019; V'lckova-Laskoska et al, 2009). It has been shown to inhibit neutrophil chemotaxis, IL-8 production, and the synthesis of inflammatory metabolites (eg, 5-lipoxygenase) (Mihara et al, 1998; Tsai and Tsai, 2019; Vuddhakul et al, 1990). Although itraconazole exerts various effects,

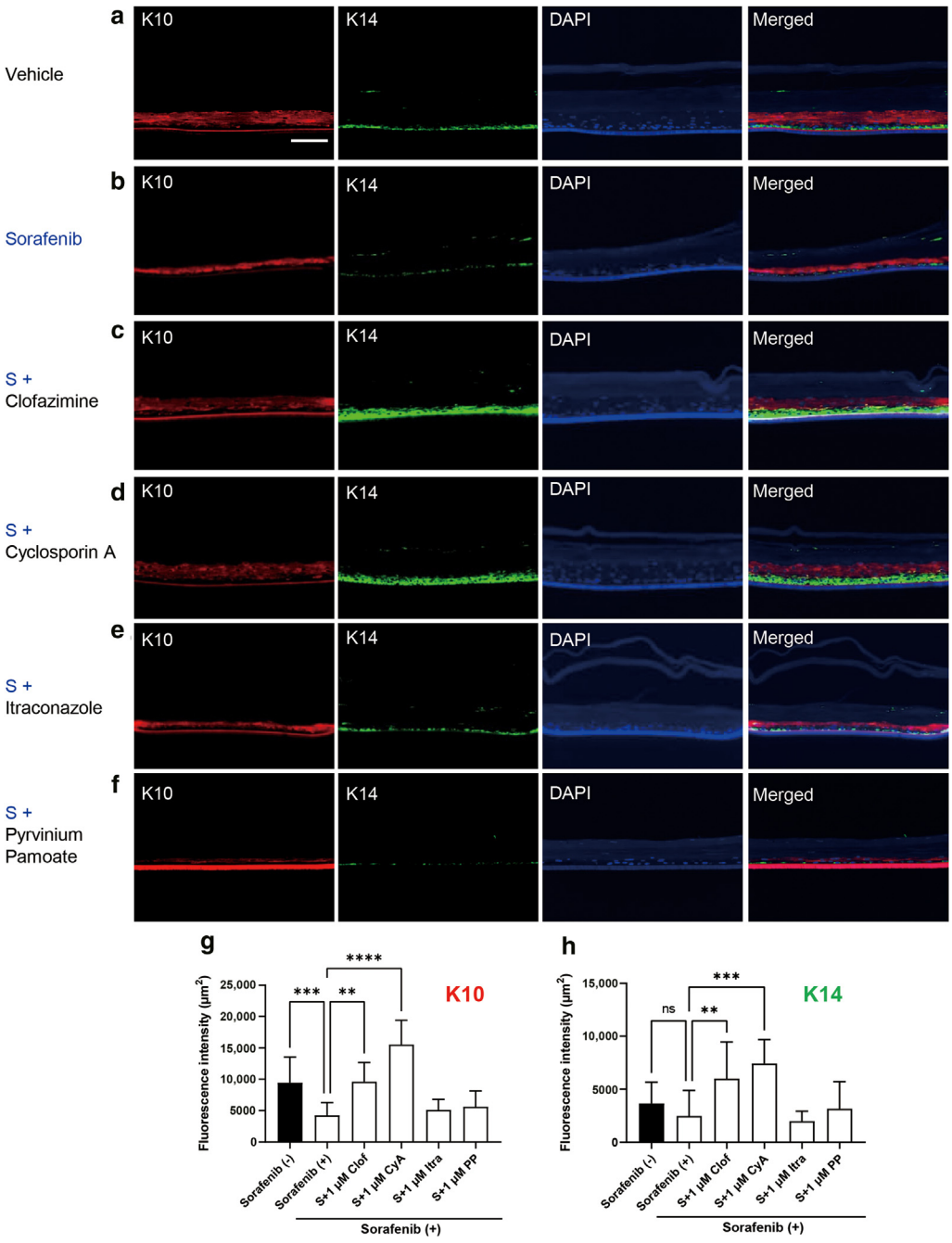

Figure 9. Immunohistochemical staining for K10 and K14 in the sorafenib- and/or hit drug–treated RHE model. (**a**–**f**) Immunohistochemistry for K10 and K14 in paraffin-embedded sections of the RHE model. Nuclei were counterstained with DAPI. Dual immunofluorescence was observed using the all-in-one fluorescence microscope BZ-X800. Bar = 100 μm. Red: K10, green: K14, and blue: DAPI (nuclei). (**g, h**) Fluorescence intensity was measured using an analysis application of the BZ-X800 series. Data were evaluated by a 1-way ANOVA followed by Tukey's test; $^{****}P < .0001$, $^{***}P < .001$, and $^{**}P < .01$. S denotes sorafenib, Clof denotes clofazimine, CyA denotes cyclosporin A, Itra denotes itraconazole, and PP denotes pyrvinium pamoate. K, keratin; ns, not significant; RHE, reconstructed human epidermis.

cytoprotection against sorafenib may be a new biological function. Itraconazole is taken mainly by oral administration, whereas other drugs, such as clotrimazole, ketoconazole, and miconazole, are by topical application (Zhang et al, 2007). Our data showed that 1 μM of other azole agents, such as bifonazole, clotrimazole, efinaconazole, isoconazole, ketoconazole, lanoconazole, luliconazole, and sulconazole, also increased cell viability in the presence of sorafenib (Figure 21a and b). Topical azole antifungal drug application may be useful to treat sorafenib-induced HFSR.

Candidate drug 4: pyrvinium pamoate

Pyrvinium pamoate is an antihelminthic drug used to treat *Enterobius vermicularis* (pinworm) (Turner and Johnson, 1962). It was recently shown to inhibit tumor cell proliferation in various cancer models, such as breast, colon, lung, and prostate cancers (Momtazi-Borojeni et al, 2018; Barbarino et al, 2018). The mechanisms underlying its anticancer effects involve (i) the suppression of energy production; (ii) inhibition of autophagy; and (iii) suppression of the Wnt–β-catenin, hedgehog, and phosphoinositide 3-kinase signaling pathways, which contribute to cell proliferation and/or tumor progression (Momtazi-Borojeni et al, 2018). Our results showed that pyrvinium pamoate markedly enhanced the viability of cultured NHEKs in the presence of sorafenib (Figure 2g). In addition, pyrvinium pamoate suppressed the sorafenib-induced apoptosis and ERK1/2 phosphorylation recovered in sorafenib-treated NHEKs. However,

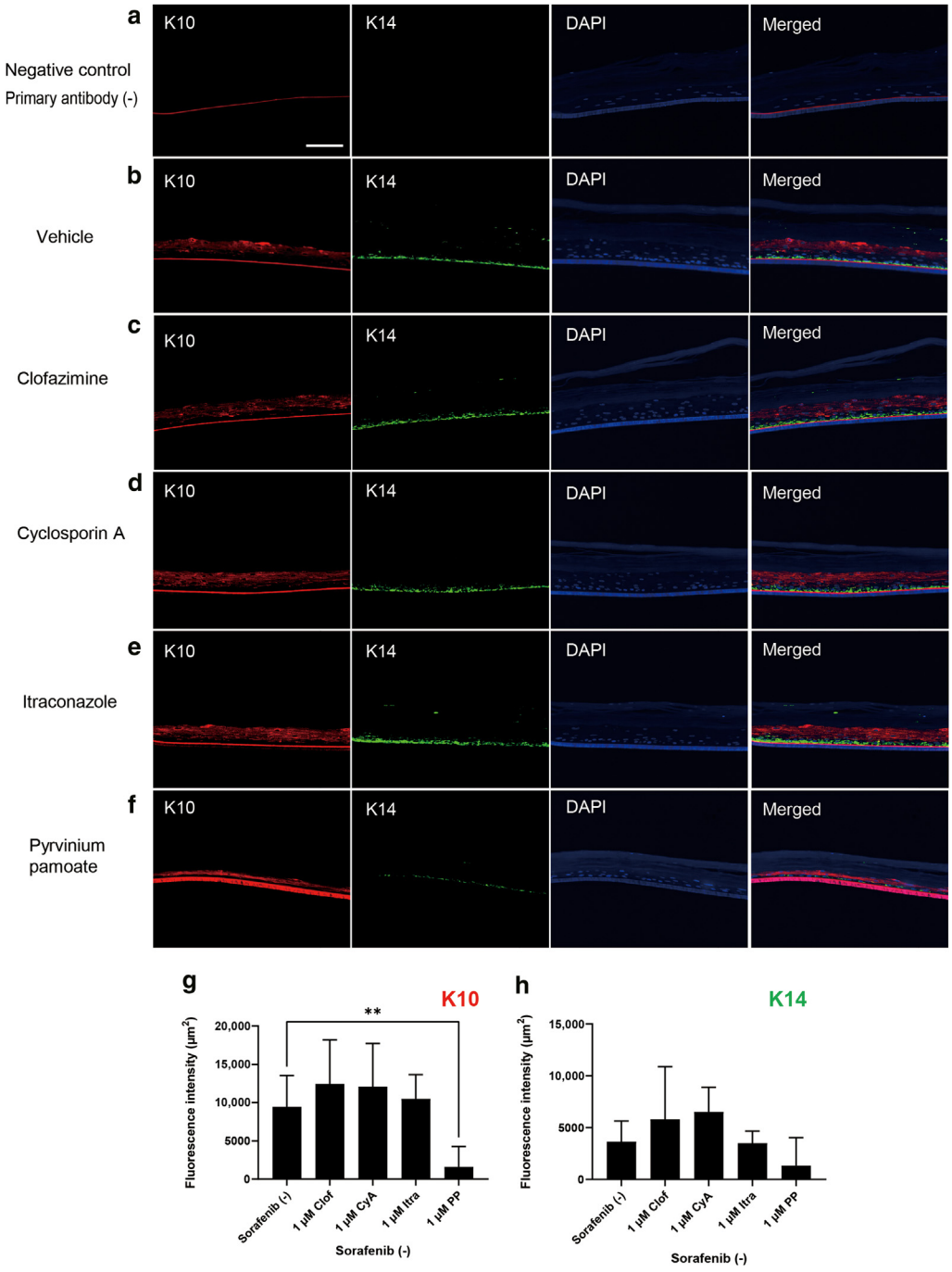

Figure 10. Immunohistochemical staining of K10 and K14 in the hit drug–treated RHE model without sorafenib. (**a**) The section without primary antibody (only secondary antibody) indicated as negative control. (**b**–**f**) Immunohistochemical image of K10 and K14 in paraffin-embedded sections of the RHE model. Nuclei were counterstained with DAPI. Dual immunofluorescence was observed by the all-in-one fluorescence microscope BZ-X800. Bar = 100 μm. (**g, h**) Fluorescence intensity was measured using an analysis application of the BZ-X800 series. The results are presented as the means ± SD of triplicate epidermisin the same experiment. Data were evaluated by a 1-way ANOVA followed by Dunnett's multiple comparison test; $^{****}P < .0001$, $^{***}P < .001$, and $^{**}P < .01$. S denotes sorafenib, Clof denotes clofazimine, CyA denotes cyclosporin A, Itra denotes itraconazole, and PP denotes pyrvinium pamoate. K, keratin; RHE, reconstructed human epidermis.

its promotion of keratinocyte proliferation in the RHE model was weaker than those of other hit drugs (Figures 7h and 9f).

Histopathological analyses of MKI-induced HFSR revealed parakeratosis, hyperkeratosis, spongiosis, the vacuolar degeneration of keratinocytes, and perivascular lymphocytic infiltration (Autier et al, 2008; Lacouture et al, 2008; Lipworth et al, 2009; Llamas-Velasco et al, 2016). These findings suggest the presence of dyskeratotic keratinocytes at various stages of necrosis in the lesional skin of patients with HFSR. In this study, the sorafenib-treated RHE model showed the vacuolation of the cytosol and nucleus in the basal and spinous layers (Figure 5e). The immunohistochemical analysis of proliferation markers, such as PCNA, revealed that sorafenib suppressed keratinocyte proliferation (Figure 7d). Therefore, sorafenib-induced skin damage may be attributed to the inhibition of epidermal keratinocyte growth. Meanwhile, epidermal differentiation marker, such as K10, loricrin, involucrin, and FLG, indicated different expression pattern after sorafenib treatment: K10 and loricrin were reduced (Figures 9a–h and 11a–h), whereas involucrin and FLG were

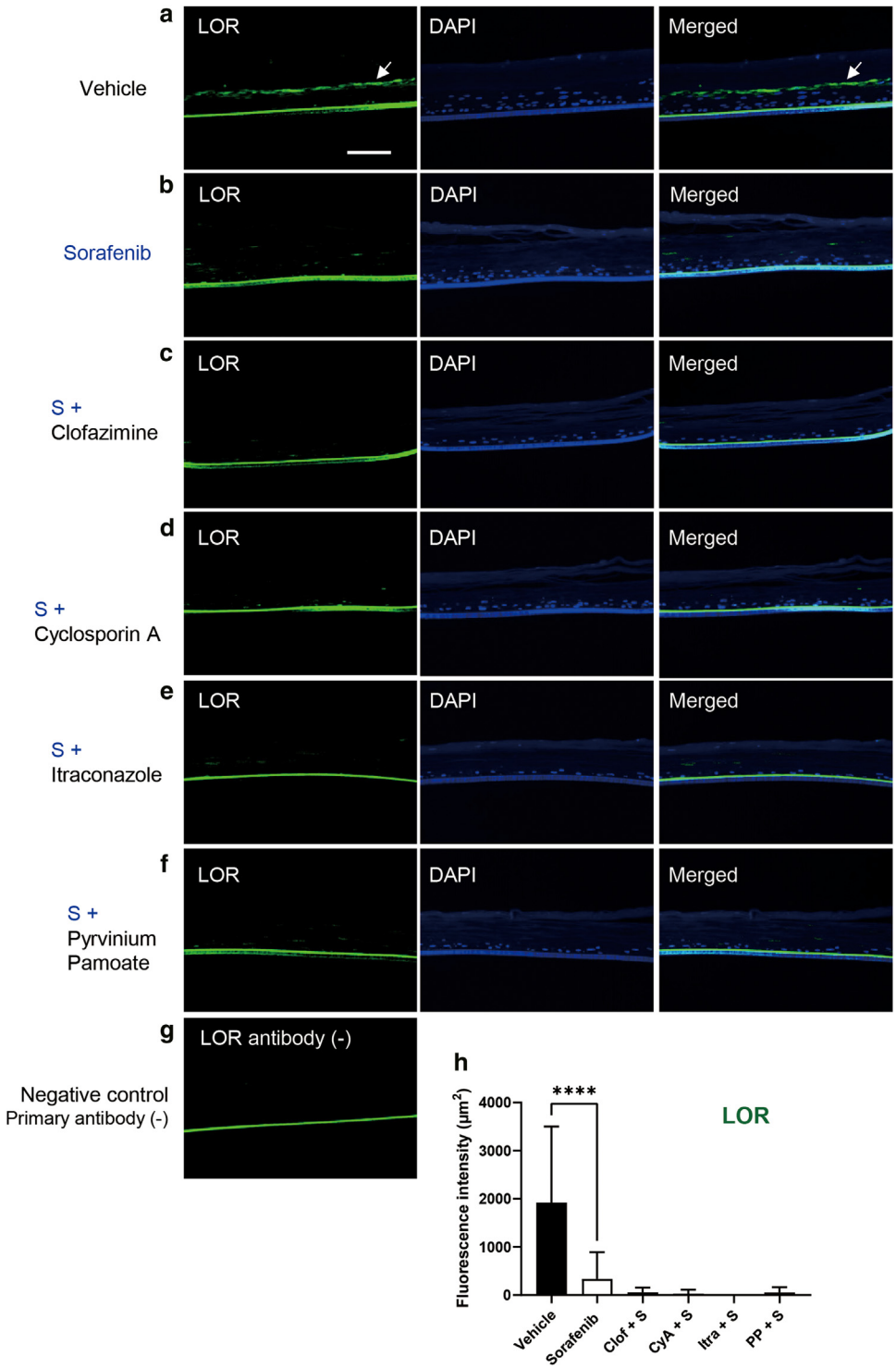

Figure 11. Immunohistochemical staining for loricrin in the sorafenib- and/or hit drug–treated RHE model. (**a**–**f**) Immunohistochemistry for loricrin in paraffin-embedded sections of the RHE model. Nuclei were counterstained with DAPI. Dual immunofluorescence was observed using the all-in-one fluorescence microscope BZ-X800. (**g**) The section without primary antibody (only secondary antibody) indicated as negative control. Bar = 100 μm. Green: loricrin, blue: DAPI (nuclei). (**h**) Fluorescence intensity was measured using an analysis application of the BZ-X800 series. The results are presented as the means ± SD of triplicate epidermis. Data were evaluated by a 1-way ANOVA followed by Tukey's test; $^{****}P <$ .0001. S denotes sorafenib, Clof denotes clofazimine, CyA denotes cyclosporin A, Itra denotes itraconazole, PP denotes pyrvinium pamoate, and LOR denotes loricrin. RHE, reconstructed human epidermis.

not changed (Figures 7a–h and 8a–h). Thus, cytotoxicity of sorafenib may be attributed to the suppression of the keratinocyte proliferation rather than to differentiation. Actually, PCNA was significantly decreased in sorafenib-treated group for RHE model (Figure 7c, d, and j). Candidate drugs, clofazimine, cyclosporin A, and itraconazole, significantly increased the number of PCNA-positive cells in the presence of sorafenib (Figure7e–g and j). Meanwhile, it has been reported that sunitinib treatment significantly decreased the expression of KRT6A in immunohistochemical staining of RHE model (Yoshida et al, 2021). However, sorafenib did not change KRT6A expression in RHE model (Figure 22a–c). It was possible that this discrepancy was caused by difference in inhibitory molecules between sorafenib and sunitinib. In

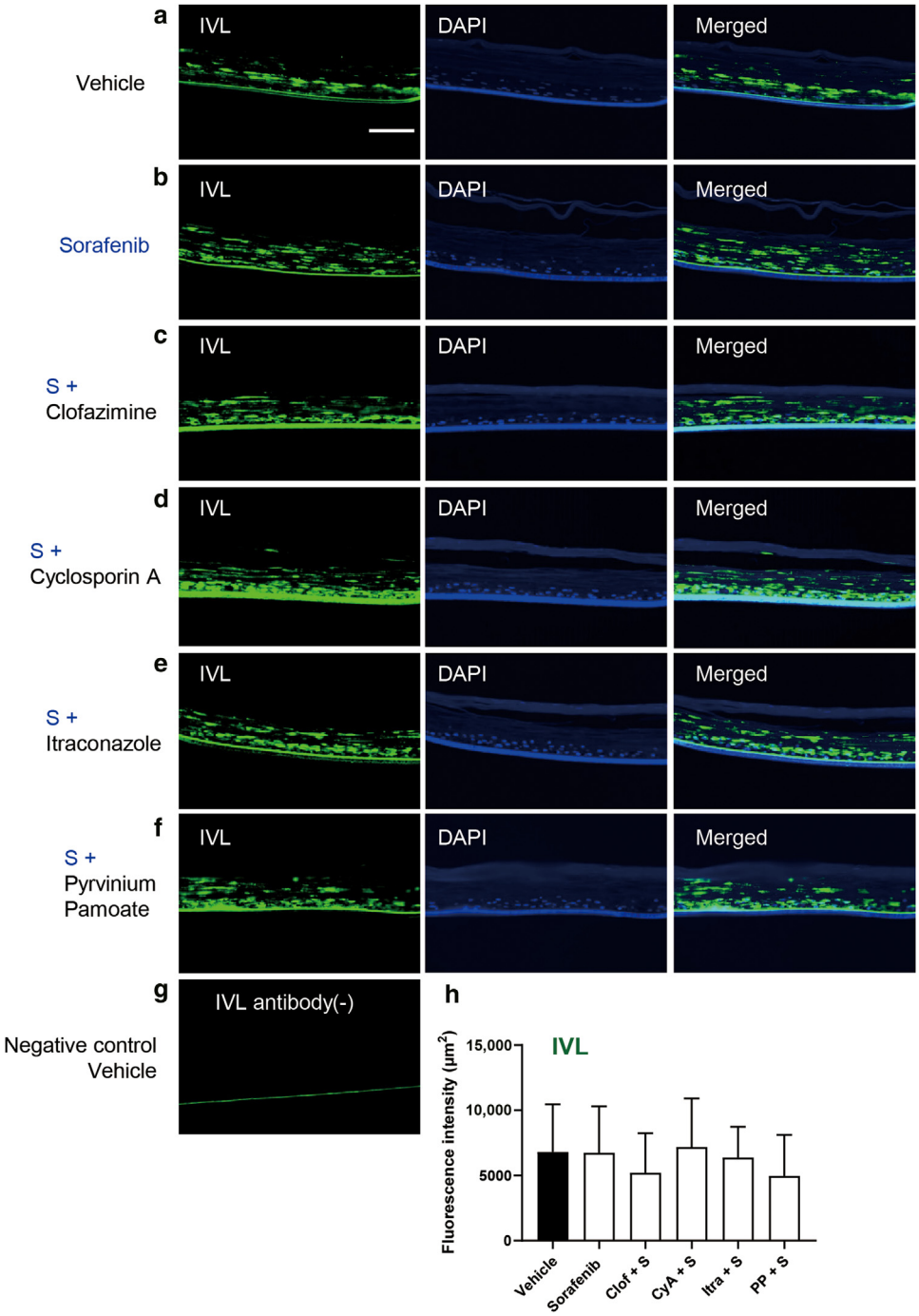

Figure 12. Immunohistochemical staining for involucrin in the sorafenib- and/or hit drug–treated RHE model. (**a**–**f**) Immunohistochemistry for involucrin in paraffin-embedded sections of the RHE model. Nuclei were counterstained with DAPI. Dual immunofluorescence was observed using the all-in-one fluorescence microscope BZ-X800. (**g**) The section without primary antibody (only secondary antibody) indicated as negative control. Bar = 100 μm. Green: involucrin, blue: DAPI (nuclei). (**h**) Fluorescence intensity was measured using an analysis application of the BZ-X800 series. The results are presented as the means ± SD of triplicate epidermis. Data were evaluated by a 1-way ANOVA followed by Tukey's test; $^{****}P <$ .0001. S denotes sorafenib, Clof denotes clofazimine, CyA denotes cyclosporin A, Itra denotes itraconazole, PP denotes pyrvinium pamoate, and IVL denote: involucrin. RHE, reconstructed human epidermis.

addition, sunitinib is reported to evoke apoptosis through Fas and FasL in mouse epidermis (Yeh et al, 2014). Our data revealed that sorafenib also induced apoptosis, whereas all candidate drugs were suppressed to increase annexin V–positive apoptotic cells (Figures 14a–g and 17a–d). Therefore, these findings showed that sorafenib toxicity on keratinocytes is mainly attributed to apoptosis.

The phosphorylation status of ERK1/2 is a useful marker for assessing Raf inhibition by sorafenib (Adnane et al, 2006). Sorafenib effectively inhibited ERK1/2 phosphorylation in NHEKs (Figure 20a and b). Interestingly, clofazimine, itraconazole, and pyrvinium pamoate significantly increased ERK1/2 phosphorylation in the presence of sorafenib. In particular, clofazimine and pyrvinium pamoate strongly recovered the phosphorylation. Cyclosporin A did not recover the decreasing phosphorylation in the presence of sorafenib (Figure 20a and b). ERK1/2 participate in cell proliferation and apoptotic inhibition. Thus, it is thought that clofazimine, itraconazole, and pyrvinium pamoate restored the suppression of ERK phosphorylation by sorafenib and

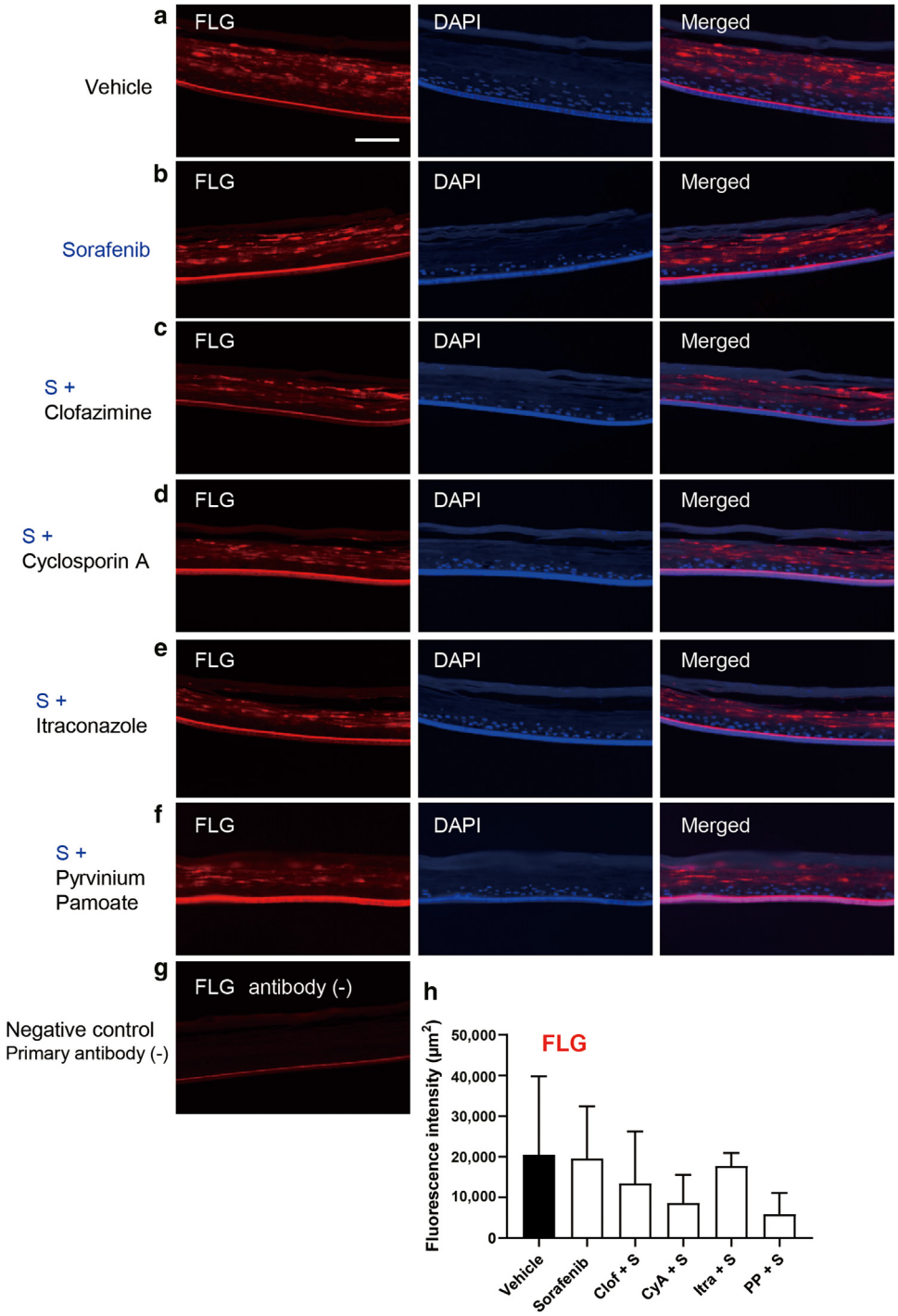

Figure 13. Immunohistochemical staining for FLG in the sorafenib- and/or hit drug–treated RHE model. (**a**–**f**) Immunohistochemistry for FLG in paraffin-embedded sections of the RHE model. Nuclei were counterstained with DAPI. Dual immunofluorescence was observed using the all-in-one fluorescence microscope BZ-X800. (**g**) The section without primary antibody (only secondary antibody) indicated as negative control. Bar = 100 μm. Red: FLG, blue: DAPI (nuclei). (**h**) Fluorescence intensity was measured using an analysis application of the BZ-X800 series. The results are presented as the means ± SD of triplicate epidermis. Data were evaluated by a 1-way ANOVA followed by Tukey's test; $^{****}P <$ .0001. S denotes sorafenib, Clof denotes clofazimine, CyA denotes cyclosporin A, Itra denotes itraconazole, and PP denotes pyrvinium pamoate. RHE, reconstructed human epidermis.

promoted the cell proliferation in NHEKs. Different mechanism may be involved in promoting cell proliferation by cyclosporin A. However, pyrvinium pamoate did not recovered PCNA and K14 expression in RHE model. In RHE model, 3-dimensional epidermal structure may be influenced by drug efficacy.

These results indicate that hit drugs, including clofazimine, cyclosporin A, itraconazole, and pyrvinium pamoate, normalize keratinocyte proliferation and protect sorafenib-induced apoptosis. In conclusion, the present results suggest the potential of these hit drugs as candidates for the treatment of MKI-induced HFSR. However, this study was performed in vitro; therefore, there are limitation for direct application of our findings to clinical practice. In future, further translational researches are required in detail.

MATERIALS AND METHODS

Chemical library

The Prestwick Chemical Library was obtained from PerkinElmer and consists of 1273 off-patent and mostly approved drugs (Food and

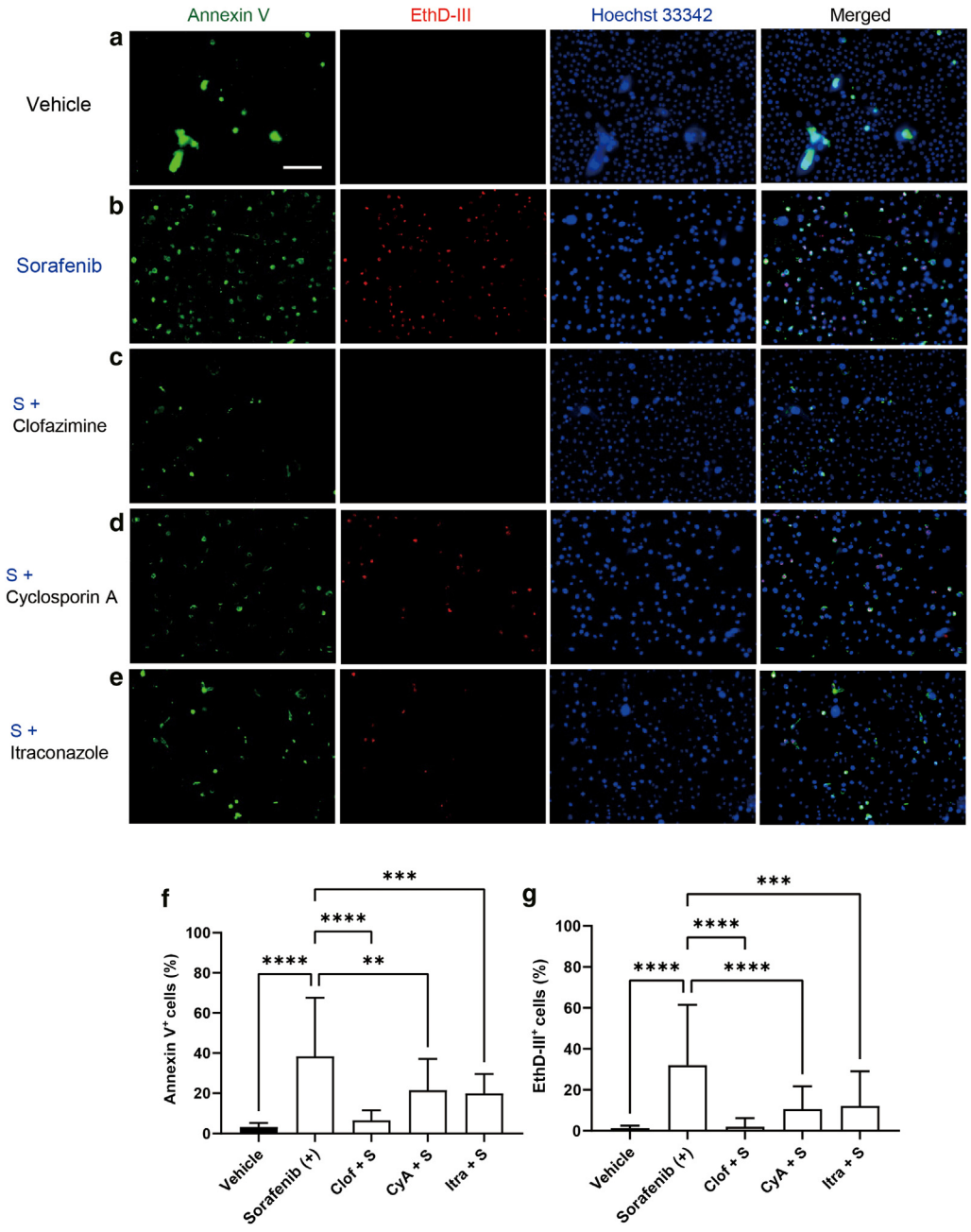

Figure 14. Apoptosis assay of sorafenib- and/or hit drug–treated NHEK. NHEKs were incubated with (**a**) DMSO (vehicle), (**b**) 7 μM sorafenib, and (**c**) 1 μM clofazimine, (**d**) cyclosporin A, or (**e**) itraconazole. After overnight incubation, the cells were stained by FITC-annexin V (green), EthD-III (red), and Hoechst 33342 (blue) and observed and analyzed by fluorescence microscope BZ-X800 and its analysis application. Cell numbers were counted in 16 random fields of view per group. (**f, g**) Relative ratio (%) of (**f**) annexin V and (**g**) EthD-III–positive cells. The results are presented as the mean ± SD. Data were evaluated by 1-way ANOVA followed by Tukey's test; $^{****}P <$ .0001, $^{***}P <$ .001, and $^{**}P <$ .01. S denotes sorafenib, Clof denotes clofazimine, CyA denotes cyclosporine A, and Itra denotes itraconazole. Bar = 100 μm. EthD-III, ethidium homodimer III; NHEK, normal human epidermal keratinocyte.

Drug Administration, European Medicines Agency, and other agencies). Compounds were predissolved at a concentration of 10 mM in DMSO.

Reagents

Avermectin B1a was from Chemscene, tolfenamic acid and N6-methyladenosine were from Namiki Shoji, bromocriptine mesylate was from Merck, and sorafenib was from Santa Cruz Biotechnology. Calcipotriene, Chicago sky blue 6B, clofazimine, cyclosporin A, halofantrine hydrochloride, itraconazole, luteolin, pyrvinium pamoate, and tolcapone were from Sigma-Aldrich. Guanfacine hydrochloride and meclozine dihydrochloride were from Tokyo Chemical Industry. All other chemicals were of reagent grade.

Primary antibodies

Antiloricrin antibody, anticytokeratin 14 rabbit mAb, and anti-involucrin antibody were obtained from Abcam. Anti-p44/42 MAPK (ERK1/2) rabbit mAb and antiphosphorylated p44/42 MAPK (ERK1/2) (Thr202/Tyr204) rabbit mAb were purchased from Cell Signaling Technology. Anti-FLG antibody was from Santa Cruz Biotechnology. Anti-K10 guinea pig polyclonal antibody was from Progen. Cytokeratin 6A polyclonal antibody and PCNA mouse mAb was from ProteinTech.

Monolayer cultures

NHEKs derived from an adult epidermis were cultured in KBM-Gold containing KGM-Gold SingleQuotes (Lonza). All cells were

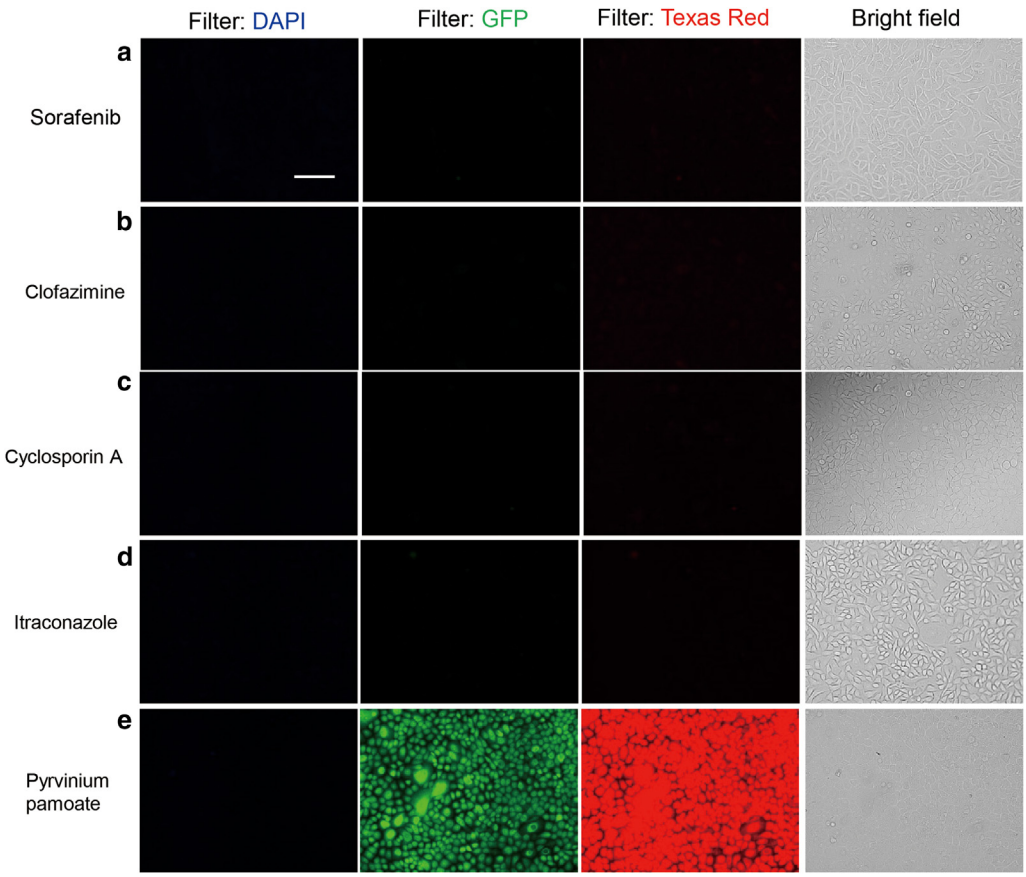

Fig. 15. Detection of autofluorescence of sorafenib and hit drugs using DAPI, GFP, and Texas Red filters. NHEKs were incubated with (**a**) 7 μM sorafenib, (**b**) 1 μM clofazimine, (**c**) cyclosporin A, (**d**) itraconazole, or (**c**) pyrvinium pamoate. After overnight incubation, the cells were observed without staining by fluorescence microscope BZ-X800. We used filters: DAPI (Ex 360 nm/Em 460 nm), GFP (Ex 470 nm/Em 525 nm), and Texas Red (Ex 560 nm/Em 630 nm). No filter: bright field. Bar = 100 μm. Em, emission wavelength; Ex, excitation wavelength; NHEK, normal human epidermal keratinocyte.

incubated at 37 °C with 5% carbon dioxide and used within 3 passages.

Screening of chemical library in NHEKs

Each chemical compound was added to subconfluent NHEKs. Cells were preincubated for 1 hour at 37 °C with chemical compound, and then both sorafenib and each drug were added to the medium and incubated overnight before performing the cell viability assay by Cell Counting Kit-8 (Dojindo Laboratories). Control, sorafenib alone, and compound alone were not preincubated. After cells were washed with PBS, Cell Counting Kit-8 solution was added to NHEKs and incubated at 37 °C for 3 hours. Cell viability was assessed by measuring absorbance at 450 nm using an ARVO X4 Multi-label Plate Reader (Perkin Elmer). In the primary screening (Figure 1), we analyzed 7 μM sorafenib + 1 μM compound and 1 μM compound alone in triplicate wells on the same plate. In the second screening (Figure 2), we performed the measurement in triplicate wells using the same plate and examined dose dependency (0.1, 1, and 10 μM). Cell viability was calculated using the following formula:

$$\text{Cell viability (\%)} = (\text{sample Abs - blank Abs}) \times 100/(\text{control Abs - blank Abs})$$

Where Abs indicate absorbance; blank indicates no cells, sorafenib (−), and compound (−); sample indicates cells (+), sorafenib (+), and compound (+); and control indicates cells (+), sorafenib (−), and compound (−).

RHE model

A 3-dimensional RHE model (EpiDerm, EPI-200) and medium (EPI-100-ASY) were obtained from MatTek. Epiderm cultures were performed according to the manufacturer's instructions. All tissues were incubated at 37 °C with 5% carbon dioxide. Briefly, the RHE model were precultured at 37 °C overnight, and tissues were exposed to medium containing both sorafenib and each candidate compound after preincubation for 1 hour at 37 °C with candidate compound. All drugs were exposed from the basal layer. After a 96-hour incubation, the MTT assay was conducted according to the manufacturer's instructions (MatTek), and the epidermal sheets were collected. All experiments were performed in triplicate wells of RHE. In addition, we checked for reproducibility with different experiments on different day.

Briefly, MTT reagent (MatTek) was added to RHE model and incubated at 37 °C. After 3 hours, RHE model was washed with PBS, isopropanol was added, and formazan was extracted for 2 hours at room temperature. After extraction, formazan extracts were moved to 96-well microplate, and absorbance was measured at 570 nm using an ARVO X4 Multi-label Plate Reader. Absorbance was measured in the wells of duplicate. Cell viability was calculated using the following formula:

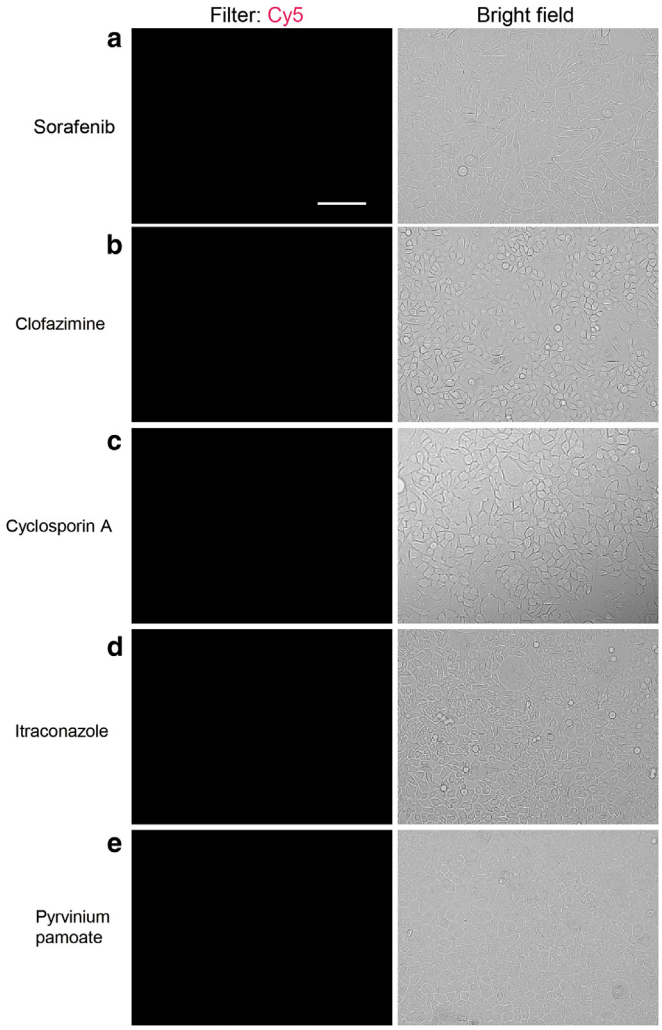

Figure 16. Detection of autofluorescence of sorafenib and hit drugs using Cy5 filter. NHEKs were incubated with (**a**) 7 μM sorafenib, (**b**) 1 μM clofazimine, (**c**) cyclosporin A, (**d**) itraconazole, or (**c**) pyrvinium pamoate. After overnight incubation, the cells were observed without staining by fluorescence microscope BZ-X800. We used filters: Cy5 (Ex 640 nm/Em 690 nm). No filter: bright field. Bar = 100 μm. Em, emission wavelength; Ex, excitation wavelength; NHEK, normal human epidermal keratinocyte.

$$\text{Cell viability (\%)} = (\text{sample Abs - blank Abs}) \times 100/(\text{control Abs - blank Abs})$$

Where Abs is absorbance; blank indicates isopropanol, sorafenib (−), and compound (−); sample indicates formazan extract (+), sorafenib (+), and compound (+); and control indicates formazan extract (+), sorafenib (−), and compound (−).

Histological analysis

The epidermis was fixed overnight in a mixture (2:1) of 4% paraformaldehyde and Superfix KY-500 (Kurabo) and embedded in 4% agar (high gel strength; Ina Kanten Karikorikan, Ina food Industry). Samples were then embedded in paraffin using the Leica TP1020 Automatic Tissue Processor (Leica Microsystems GmbH) and tissue embedding system (Ogawa Seiki). Samples were cut into 4-μm-thick paraffin sections using the retoratome REM-710 (Yamato Kohki Industrial) and mounted onto silane-coated glass slides. Sections were deparaffinized, rehydrated, and analyzed by H&E staining.

Proliferating cells were detected by immunohistochemical staining for PCNA. Paraffin sections were deparaffinized and rehydrated, followed by antigen retrieval at 110 °C for 10 minutes using antigen retrieval buffer (citrate buffer, pH 6.0) (Abcam) and the decloaking chamber NxGen (Biocare Medical). After washing with PBS, endogenous peroxidase blocking was conducted at room temperature for 10 minutes using hydrogen peroxide−blocking reagent (Abcam), followed by washing with PBS containing 0.2% Tween 20 (PBST) and incubation at room temperature for 1 hour with blocking solution (PBS containing 2% BSA, 5% normal goat serum, and 0.2% Triton X-100). After blocking, sections were incubated at 4 °C overnight with a PCNA mouse mAb (1:1000 dilution). On the next day, sections were washed with PBST and incubated at room temperature for 1 hour with goat anti-mouse IgG H&L (horseradish peroxidase polymer) (Abcam). After washing with PBST, sections were treated using the 3,3′- diaminobenzidine substrate kit (Abcam) at room temperature, counterstained with Mayer's hematoxylin, dehydrated with ethanol, cleared with xylene, and mounted.

K10 and K14 were detected by immunofluorescence staining. Paraffin sections were deparaffinized and rehydrated, and antigen

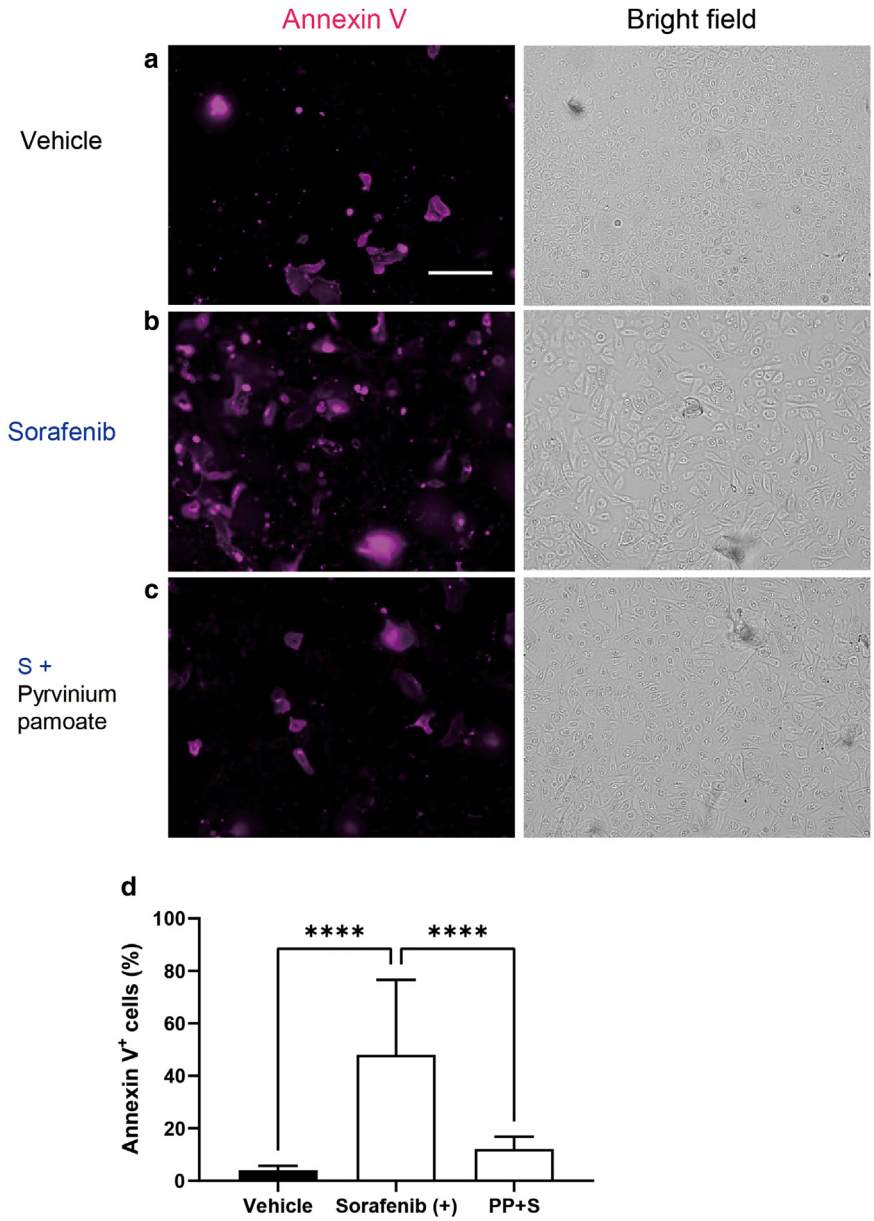

Figure 17. Apoptosis assay of sorafenib- and/or pyrvinium pamoate −treated NHEK. NHEKs were incubated with (**a**) DMSO (vehicle), (**b**) 7 μM sorafenib, and/or (**c**) 1 μM pyrvinium pamoate. After overnight incubation, the cells were stained by Annexin V−conjugated Alexa Fluor 647 (violet) and observed and analyzed by fluorescence microscope BZ-X800 and its analysis application. Annexin V−positive cell numbers were counted in 16 random fields of view per group. The number of whole cells in a bright field was counted by manual handling. (**d**) Relative ratio (%) of annexin V−positive cells. The results were presented as the mean ± SD. Data were evaluated by 1-way ANOVA followed by Tukey's test; $^{****}P < .0001$. S denotes sorafenib, and PP denotes pyrvinium pamoate. Bar = 100 μm. NHEK, normal human epidermal keratinocyte.

retrieval was performed at 110 °C for 10 minutes using antigen retrieval buffer (citrate buffer, pH 6.0) (Abcam) and the decloaking chamber NxGen (Biocare Medical). After washing with PBST, sections were incubated at room temperature for 1 hour with blocking solution (PBS containing 2% BSA, 5% normal donkey serum, and 0.2% Triton X-100) and then with an anti-K10 guinea pig polyclonal antibody (1:200 dilution), anticytokeratin 14 rabbit mAb (1:2000 dilution), antiloricrin (1:500 dilution), anti-involucrin (1:150 dilution), anti-FLG (1:200 dilution), and anti-KRT6A (1:500 dilution) at 4 °C overnight. K10 and K14 were costained in the same section. On the next day, sections were washed with PBST and incubated at room temperature for 1 hour with a donkey anti-rabbit IgG (H+L) highly cross-adsorbed secondary antibody conjugated with Alexa Fluor 488 (1:300 dilution, Thermo Fisher Scientific), donkey anti-guinea pig IgG (H+L), AffiniPure F(ab')$_2$ Fragment−conjugated Alexa Fluor 594 (1:300 dilution, Jackson ImmunoResearch Laboratories), and/or donkey anti-mouse IgG (H+L) highly cross-adsorbed secondary antibody conjugated with Alexa Fluor 594 (1:300 dilution, Thermo Fisher Scientific). After washing with PBST, sections were mounted using Vectashield Mounting Medium with DAPI.

A morphological analysis by H&E staining and immunohistochemistry was performed using the all-in-one fluorescence microscope BZ-X800 (Keyence). PCNA-positive nuclei were manually counted and indicated as a relative value (%) to all nuclei. The fluorescence intensity and area of vacuoles were measured in at least 9 images from each group using an analysis application in the BZ-X800 series (Keyence).

Apoptosis assay

Annexin V−positive apoptotic cells were detected using Apoptotic, Necrotic and Healthy Cells Quantification Kit (Biotium). After preincubation for 1 hour at 37 °C with candidate drug, sorafenib (7 μM)

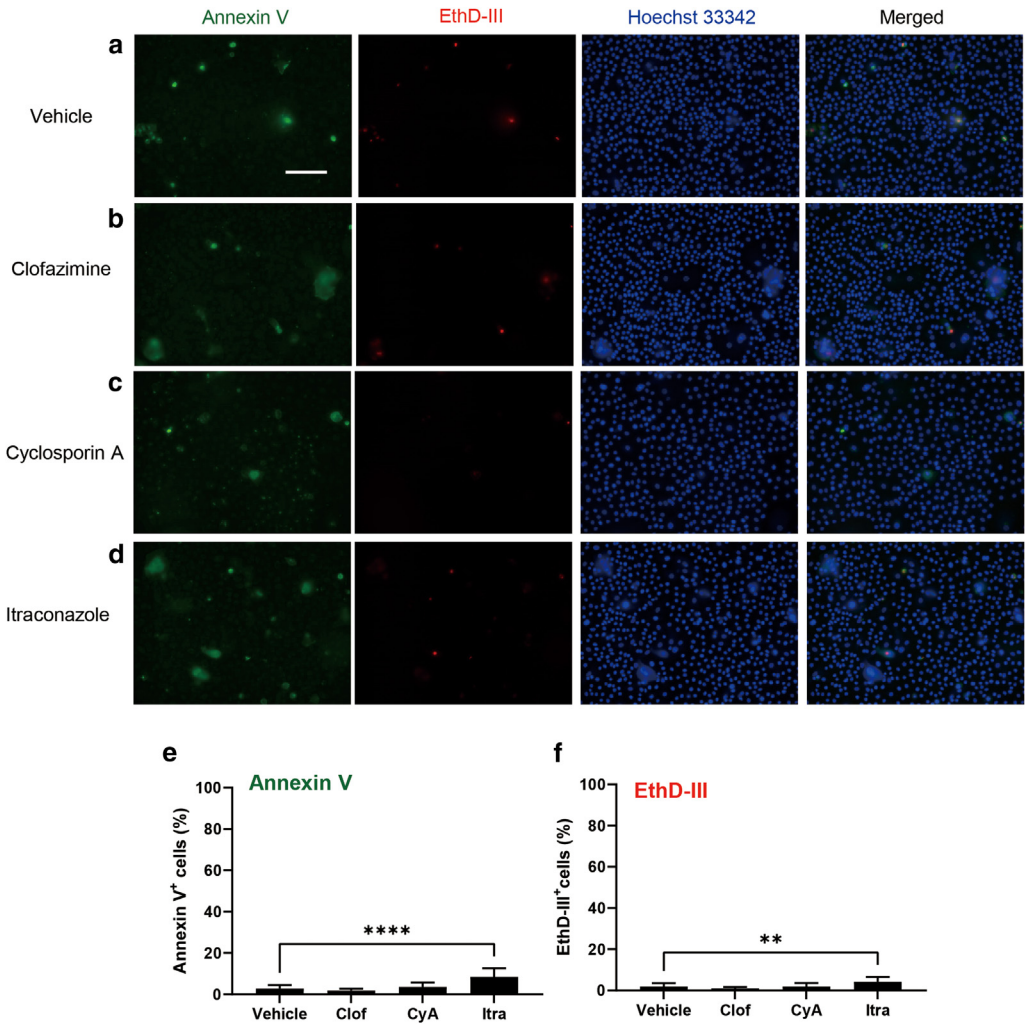

Figure 18. Apoptosis assay of hit drugs treated NHEK. NHEKs were incubated with (**a**) DMSO (vehicle), (**b**) 1 μM clofazimine, (**c**) cyclosporin A, or (**d**) itraconazole. After overnight incubation, the cells were stained by FITC-annexin V (green), EthD-III (red), and Hoechst 33342 (blue) and observed and analyzed by fluorescence microscope BZ-X800 and its analysis application. Cell numbers were counted in 16 random fields of view per group. (**e, f**) Relative ratio (%) of (**f**) annexin V− and (**g**) EthD-III−positive cells. The results are presented as the means ± SD. Data were evaluated by 1-way ANOVA followed by Dunnett's test; $^{****}P <$ .0001 and $^{**}P <$ .01. Clof denotes clofazimine, CyA denotes cyclosporine A, and Itra denotes itraconazole. Bar = 100 μm. EthD-III, ethidium homodimer III; NHEK, normal human epidermal keratinocyte.

and clofazimine, cyclosporine A or itraconazole (1 μM) was added to subconfluent keratinocytes and incubated for overnight. Cells were washed twice with PBS and 1x binding buffer, respectively. Next, 1x binding buffer containing FITC-annexin V, EthD-III, and Hoechst 33342 was added, and the cells were incubated at room temperature in the dark for 15 minutes. Then, the cells were washed twice with 1x binding buffer, covered with a cover glass, and imaged by BZ-X800 fluorescence microscope (Keyence). The numbers of stained cell were counted by BZ-X analyzer (Keyence). Relative ratio of annexin V− and EthD-III−positive cells were calculated using the following formulae:

For relative ratio (%) of annexin V−positive cells : annexin V^+ cells × 100/Hoechst 33342^+ cells.

For relative ratio(%)of EthD-III−positive cells : EthD-III^+ cells × 100/Hoechst 33342^+ cells

As other methods, annexin V−positive cells were detected using Alexa Fluor 647−conjugated annexin V (Thermo Fisher Scientific). After preincubation for 1 hour at 37 °C with pyrvinium pamoate, sorafenib (7 μM) and/or pyrvinium pamoate (1 μM) was added to subconfluent keratinocytes and incubated for overnight. Cells were washed twice with PBS and binding buffer (10 mM 4-[2-hydroxyethyl]-1-piperazineethanesulfonic acid, 0.14 M sodium chloride, and 2.5 mM calcium chloride, pH 7.4). Next, binding buffer containing Alexa Fluor 647−conjugated annexin V was added, and the cells were incubated at room temperature in the dark for 15 minutes. Then, the cells were washed twice with binding buffer, covered with a cover glass, and imaged by BZ-X800 fluorescence microscope (Keyence). The numbers of annexin V−positive cell were counted by BZ-X analyzer (Keyence), and the numbers of whole cell in bright field were counting by manual handling. Relative ratio of annexin V−positive cells were calculated using the following formula:

For relative ratio (%) of annexin V−positive cells, annexin V^+ cells × 100/whole cell numbers

Autofluorescence of each drugs was validated in the absence of annexin V, EthD-III, and Hoechst 33342. Filters used DAPI (excitation wavelength 360 nm/emission wavelength 460 nm, for Hoechst33342), GFP (excitation wavelength 470 nm/emission

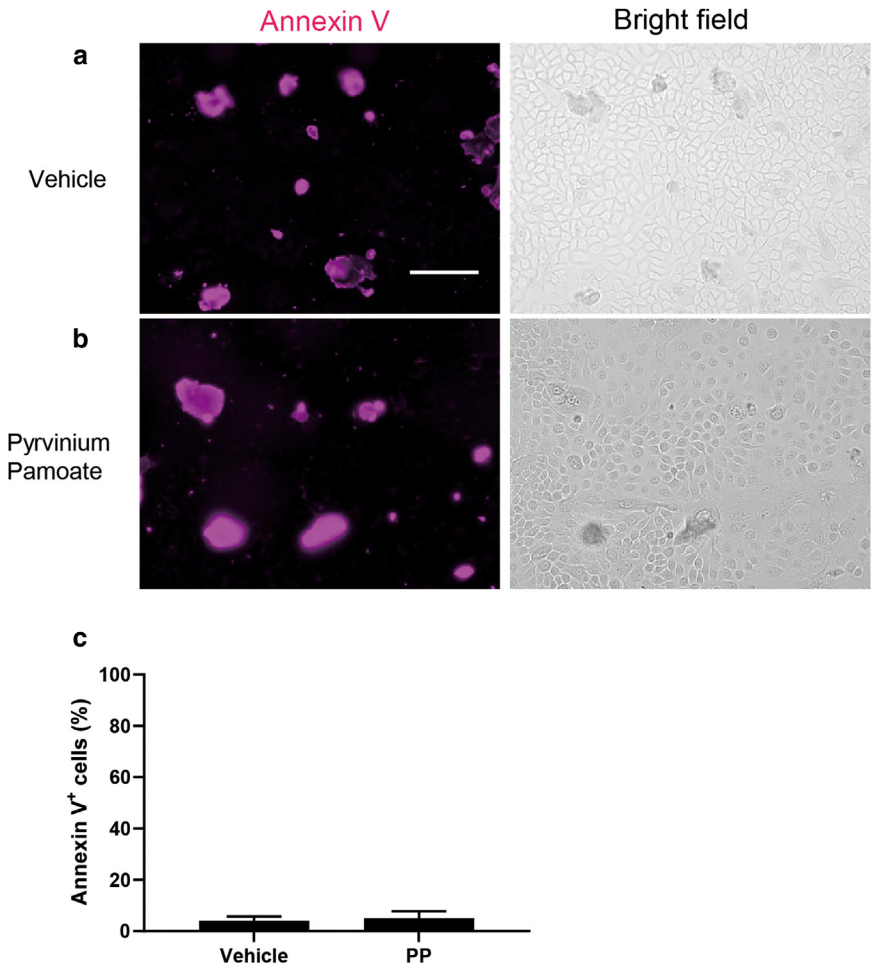

Figure 19. Apoptosis assay of pyrvinium pamoate treated NHEK. NHEKs were incubated with (**a**) DMSO (vehicle) and (**b**) 1 μM pyrvinium pamoate. After overnight incubation, the cells were stained by annexin V–conjugated Alexa Fluor 647 (violet) and observed and analyzed by fluorescence microscope BZ-X800 and its analysis application. Annexin V–positive cell numbers were counted in 16 random fields of view per group. The number of whole cells in a bright field was counted by manual handling. (**f**) Relative ratio (%) of annexin V–positive cells. The results are presented as the means ± SD. Data were evaluated by 1-way ANOVA followed by Dunnett's test. S denotes sorafenib, and PP denotes pyrvinium pamoate. Bar = 100 μm. NHEK, normal human epidermal keratinocyte.

wavelength 525 nm, for FITC-Annexin V), Texas Red (excitation wavelength 560 nm/emission wavelength 630 nm, for EthD-III), and Cy5 (excitation wavelength 640 nm/emission wavelength 690 nm, for Annexin V–conjugated Alexa Fluor 647) (Keyence).

Western blotting

After preincubation for 1 hour at 37 °C with 1 μM candidate compound, NHEKs were incubated for 1 hour at 37 °C with DMSO (vehicle); 7 μM sorafenib; and 1 μM clofazimine, cyclosporin A, itraconazole, or pyrvinium pamoate. The cell lysates were prepared using M-PER mammalian protein extraction reagent (Thermo Fisher Scientific) containing Halt protease inhibitor cocktail and Halt phosphatase inhibitor cocktail (Thermo Fisher Scientific).

Equal amounts of total protein (5 μg) of cell lysate were applied to e-PAGEL 10% (ATTO) and electrophoresed for 70 minutes at 20 mA/gel. After electrophoresis, proteins were transferred onto an Immobilon-P PVDF membrane (Millipore) by Powered Blot (ATTO). The membrane was blocked with EzBlock Chemi (ATTO) at room temperature for 1 hour and then incubated with primary antibody (anti-ERK1/2 [1:2000 dilution] or antiphosphorylated ERK1/2 [1:1000 dilution]) overnight at 4 °C. The next day, the membranes were washed three times with Tris-buffered saline with Tween 20 and then incubated with horseradish peroxidase–conjugated goat anti-rabbit IgG (H+L), superclonal recombinant secondary antibody (1:10,000 dilution) for 1 hour at room temperature. After washing three times with Tris-buffered saline with Tween 20, bands were detected with SuperSignal West Pico PLUS Chemiluminescent Substrate (Thermo Fisher Scientific) using Amersham Imager 600 (GE Healthcare). Anti–β-actin (1:5000 dilution) (ProteinTech) was used as an internal control. Relative densities of bands were analyzed by National Institutes of Health ImageJ program.

Statistical analysis

We used a 1-way ANOVA with Dunnett's or Tukey's multiple comparison tests. All statistical analyses were performed using GraphPad Prism 9 (GraphPad Software).

ETHICS STATEMENT

No human or mice studies were performed.

DATA AVAILABILITY STATEMENT

The datasets analyzed in this study are available from the corresponding author on reasonable request.

ORCIDs

Yayoi Kamata: http://orcid.org/0000-0002-3477-5715
Rui Kato: http://orcid.org/0000-0002-5967-3889
Mitsutoshi Tominaga: http://orcid.org/0000-0002-1254-1803
Sumika Toyama: http://orcid.org/0000-0003-3606-245X
Eriko Komiya: http://orcid.org/0000-0002-7450-1188
Jun Utsumi: http://orcid.org/0000-0003-2632-9325

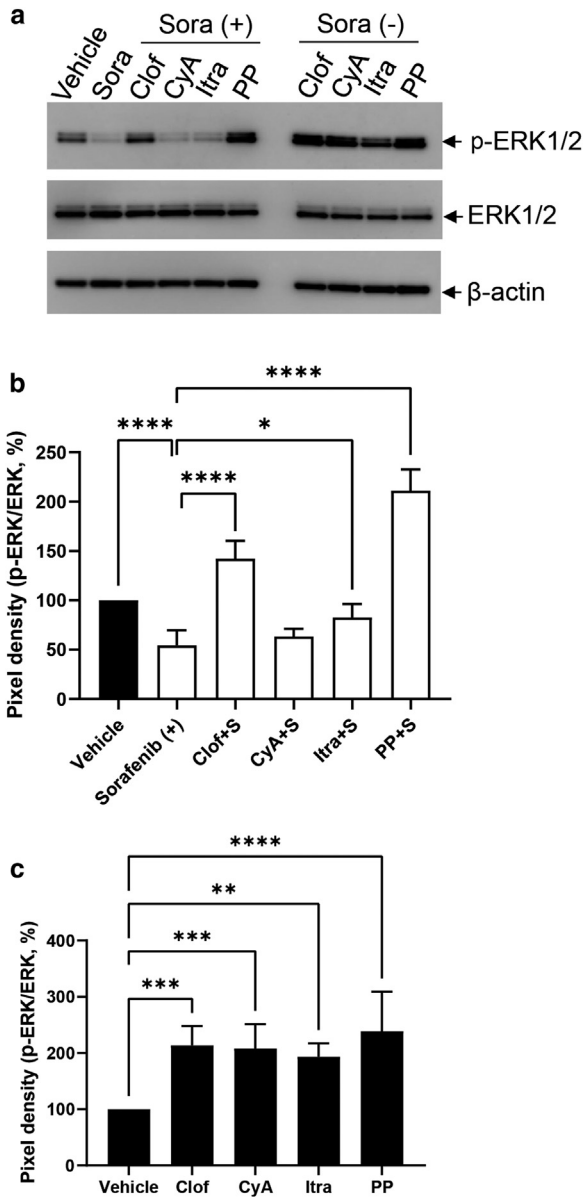

Figure 20. Western blot analysis of ERK1/2 phosphorylation in NHEKs. NHEKs were incubated with DMSO (vehicle), 7 μM sorafenib, 1 μM clofazimine, cyclosporin A, itraconazole, or pyrvinium pamoate. After preincubation for 1 h, the cell lysates were prepared, and western blotting was performed. (**a**) Western blot images of the p-ERK1/2, ERK1/2, and β-actin (internal control). Protein contents of all samples were set at 5 μg/lane. (**b, c**) Bands were semiquantified by ImageJ. Data were indicated as a relative ratio of p-ERK/ERK. The results are presented as the mean ± SD of separately triplicate experiments. Data were evaluated by 1-way ANOVA followed by Tukey's test; $^{****}P < .0001$, $^{***}P < .001$, $^{**}P < .01$, and $^{*}P < .05$. S denotes sorafenib, Clof denotes clofazimine, CyA denotes cyclosporin A, and PP denotes pyrvinium pamoate. ERK, extracellular signal–regulated kinase; h, hour; NHEK, normal human epidermal keratinocyte; p-ERK, phosphorylated extracellular signal–regulated kinase.

Takahide Kaneko: http://orcid.org/0000-0002-6219-6665
Yasushi Suga: http://orcid.org/0000-0003-3643-2879
Kenji Takamori: http://orcid.org/0000-0002-0644-0504

CONFLICT OF INTEREST

YK received a research scholarship from Maruho. KT received a research grant from TORAY Industries. The remaining authors state no conflict of interest.

DECLARATION OF GENERATIVE ARTIFICIAL INTELLIGENCE (AI) OR LARGE LANGUAGE MODELS (LLMs)

The authors did not use the generative intelligence or large language models in the writing process.

ACKNOWLEDGMENTS

We would like to thank A. Kajita for her technical support in this research. We also thank M. Fujishiro for her technical advice for histopathology. This work was partly supported by a research scholarship from Maruho (Osaka, Japan) and a research grant from TORAY Industries (Tokyo, Japan).

AUTHOR CONTRIBUTIONS

Conceptualization: YK, MT, JU; Data Curation: YK, MT; Formal Analysis: YK, RK; Funding Acquisition: YK, KT; Investigation: YK, RK, ST, EK; Methodology: YK, MT, JU; Project Administration: YK, MT, KT; Resources: YK, RK, MT, TK, YS, KT; Supervision: MT, KT; Validation: YK, RK; Visualization: YK, RK, ST, EK; Writing - Original Draft Preparation: YK, MT; Writing - Review and Editing: TK, YS, KT

Table 2. Cell Viability in the Presence of 1 μM of CYP3A4 Inhibitors with 7 μM Sorafenib

ID	Chemical Name	Therapeutic Effect	Cell Viability (%)	*P*-Value[1]
Strong CYP3A4 inhibitors				
08A08	Itraconazole	Antifungal	209.8 ± 20.5	.0007***
04F10	Mifepristone	Abortifacient	128.5 ± 22.0	n.s
05G10	Ketoconazole	Antifungal	123.0 ± 75.1	n.s
16F03	Indinavir	Antiviral	114.8 ± 19.7	n.s
16F11	Ritonavir	Antiviral	114.8 ± 20.6	n.s
15E09	Clarithromycin	Antibacterial	106.2 ± 6.4	n.s
08C06	Voriconazole	Antifungal	95.9 ± 11.9	n.s
16A02	Nelfinavir	Antiviral	90.6 ± 10.3	n.s
14H05	Saquinavir	Antiviral	87.7 ± 10.6	n.s

Abbreviations: ID, identification; n.s, not significant.
All results are presented as the mean ± SD of triplicate wells in the single plate. ***$P < .001$.
[1]Student's *t*-test (vs vehicle with 7 μM sorafenib).

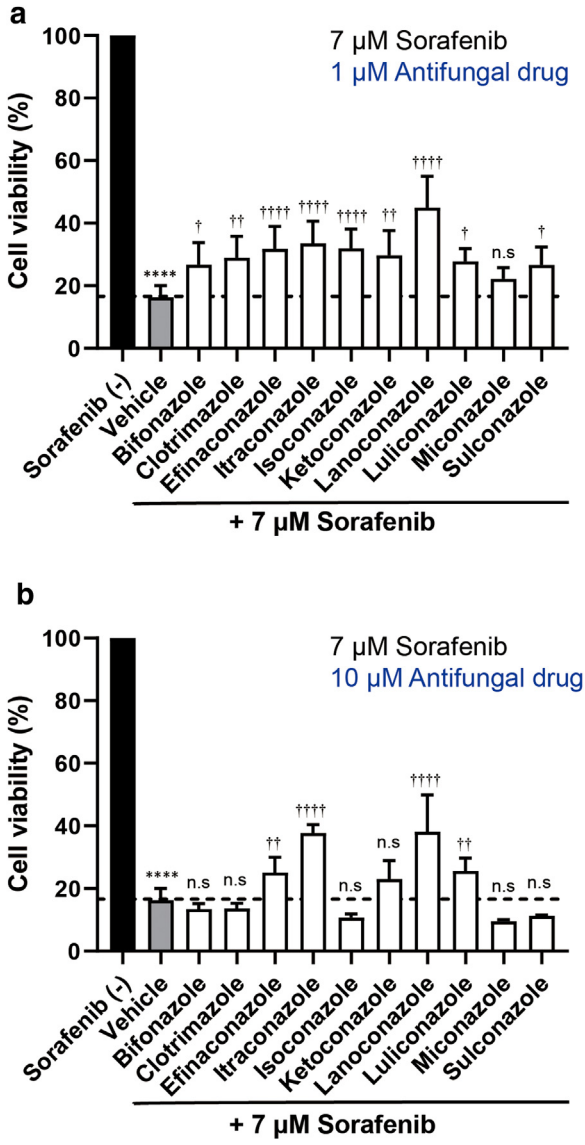

Figure 21. Effect of azole antifungal drugs against sorafenib toxicity in NHEKs. NHEKs were incubated at 37 °C overnight with (**a**) 1 μM or (**b**) 10 μM azole antifungal agent in the presence of 7 μM sorafenib. Cell viability was assessed by CCK-8 assay. The dashed lines indicate 17% cell viability with a single treatment of 7 μM sorafenib. Data were evaluated using 1-way ANOVA followed by Tukey's test; $^{****}P < .0001$ (vs vehicle without sorafenib) and $^{††††}P < .0001$, $^{††}P < .01$, and $^{†}P < .05$ (vs vehicle in the presence of 7 μM sorafenib). All results are presented as the means ± SD of triplicate experiments. CCK-8, Cell Counting Kit-8; NHEK, normal human epidermal keratinocyte; ns, not significant.

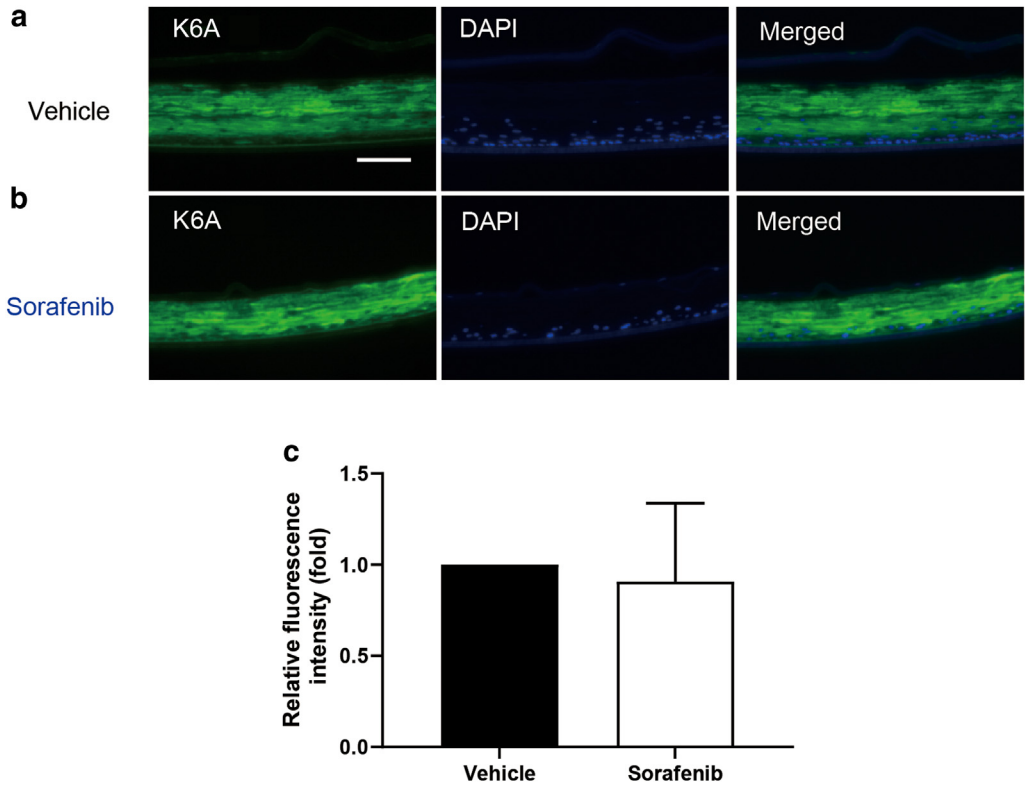

Figure 22. Immunohistochemical staining for K6A in sorafenib-treated RHE model. (**a, b**) Immunohistochemistry for K6A in paraffin-embedded sections of the RHE model. Nuclei were counterstained with DAPI. Dual immunofluorescence was observed using the all-in-one fluorescence microscope BZ-X800. Bar = 100 μm. Green: K6A, blue: DAPI (nuclei). (**c**) Fluorescence intensity was measured using an analysis application of the BZ-X800 series. The results are presented as the means ± SD of triplicate epidermis. Data were evaluated by a 1-way ANOVA followed by Student's *t*-test. K6A, keratin 6A; RHE, reconstructed human epidermis.

REFERENCES

Adnane L, Trail PA, Taylor I, Wilhelm SM. Sorafenib (BAY 43-9006, Nexavar), a dual-action inhibitor that targets RAF/MEK/ERK pathway in tumor cells and tyrosine kinases VEGFR/PDGFR in tumor vasculature. Methods Enzymol 2006;407:597–612.

Ahmadi A, Mohammadnejadi E, Karami P, Razzaghi-Asl N. Current status and structure activity relationship of privileged azoles as antifungal agents (2016–2020). Int J Antimicrob Agents 2022;59:106518.

Amor KT, Ryan C, Menter A. The use of cyclosporine in dermatology: part I. J Am Acad Dermatol 2010;63:925–46. quiz 947.

Ancker OV, Krüger M, Wehland M, Infanger M, Grimm D. Multikinase inhibitor treatment in thyroid cancer. Int J Mol Sci 2019;21:10.

Arbiser JL, Moschella SL. Clofazimine: a review of its medical uses and mechanisms of action. J Am Acad Dermatol 1995;32:241–7.

Autier J, Escudier B, Wechsler J, Spatz A, Robert C. Prospective study of the cutaneous adverse effects of sorafenib, a novel multikinase inhibitor. Arch Dermatol 2008;144:886–92.

Azzi JR, Sayegh MH, Mallat SG. Calcineurin inhibitors: 40 years later, can't live without. J Immunol 2013;191:5785–91.

Barbarino M, Cesari D, Intruglio R, Indovina P, Namagerdi A, Bertolino FM, et al. Possible repurposing of Pyrvinium pamoate for the treatment of mesothelioma: a pre-clinical assessment. J Cell Physiol 2018;233:7391–401.

Cabanillas ME, Ryder M, Jimenez C. Targeted therapy for advanced thyroid cancer: kinase inhibitors and beyond. Endocr Rev 2019;40:1573–604.

Carlomagno F, Anaganti S, Guida T, Salvatore G, Troncone G, Wilhelm SM, et al. BAY 43-9006 inhibition of oncogenic RET mutants. J Natl Cancer Inst 2006;98:326–34.

Cholo MC, Steel HC, Fourie PB, Germishuizen WA, Anderson R. Clofazimine: current status and future prospects. J Antimicrob Chemother 2012;67:290–8.

Grandinetti CA, Goldspiel BR. Sorafenib and sunitinib: novel targeted therapies for renal cell cancer. Pharmacotherapy 2007;27:1125–44.

Grothey A, Van Cutsem E, Sobrero A, Siena S, Falcone A, Ychou M, et al. Regorafenib monotherapy for previously treated metastatic colorectal cancer (CORRECT): an international, multicentre, randomised, placebo-controlled, phase 3 trial. Lancet 2013;381:303–12.

Kanda N, Kano R, Ishikawa T, Watanabe S. The antimycotic drugs itraconazole and terbinafine hydrochloride induce the production of human μ-defensin-3 in human keratinocytes. Immunobiology 2011;216:497–504.

Kobayashi K, Kawakami K, Yokokawa T, Aoyama T, Suzuki K, Wakatsuki T, et al. Association of hand-foot skin reaction with regorafenib efficacy in the treatment of metastatic colorectal cancer. Oncology 2019;96:200–6.

Krishnamoorthy SK, Relias V, Sebastian S, Jayaraman V, Saif MW. Management of regorafenib-related toxicities: a review. Therap Adv Gastroenterol 2015;8:285–97.

Lacouture ME, Reilly LM, Gerami P, Guitart J. Hand foot skin reaction in cancer patients treated with the multikinase inhibitors sorafenib and sunitinib. Ann Oncol 2008;19:1955–61.

Lavoie H, Gagnon J, Therrien M. ERK signalling: a master regulator of cell behaviour, life and fate. Nat Rev Mol Cell Biol 2020;21:607–32.

Lipworth AD, Robert C, Zhu AX. Hand-foot syndrome (hand-foot skin reaction, palmar-plantar erythrodysesthesia): focus on sorafenib and sunitinib. Oncology 2009;77:257–71.

Llamas-Velasco M, Hegyi I, Hesterberg U, Daudén E, Requena L, Kempf W. Regorafenib-induced hand-foot skin reaction with striking epidermal dysmaturation - a new histopathological pattern associated with the use of multi-kinase inhibitors. Br J Dermatol 2016;175:216–7.

Llovet JM, Montal R, Sia D, Finn RS. Molecular therapies and precision medicine for hepatocellular carcinoma. Nat Rev Clin Oncol 2018;15:599–616.

McLellan B, Ciardiello F, Lacouture ME, Segaert S, Van Cutsem E. Regorafenib-associated hand-foot skin reaction: practical advice on diagnosis, prevention, and management. Ann Oncol 2015;26:2017–26.

Mihara M, Hagari Y, Morimura T, Nakayama H, Isihara M, Aki T, et al. Itraconazole as a new treatment for pustulosis palmaris et plantaris. Arch Dermatol 1998;134:639–40.

Momtazi-Borojeni AA, Abdollahi E, Ghasemi F, Caraglia M, Sahebkar A. The novel role of Pyrvinium in cancer therapy. J Cell Physiol 2018;233:2871–81.

Ryan C, Amor KT, Menter A. The use of cyclosporine in dermatology: part II. J Am Acad Dermatol 2010;63:949–72. quiz 973.

Saag MS, Dismukes WE. Azole antifungal agents: emphasis on new triazoles. Antimicrob Agents Chemother 1988;32:1–8.

Stanculeanu DL, Zob D, Toma OC, Georgescu B, Papagheorghe L, Mihaila RI. Cutaneous toxicities of molecular targeted therapies. Maedica (Bucur) 2017;12:48–54.

Sugita T, Miyamoto M, Tsuboi R, Takatori K, Ikeda R, Nishikawa A. In vitro activities of azole antifungal agents against Propionibacterium acnes isolated from patients with acne vulgaris. Biol Pharm Bull 2010;33:125–7.

Tsai YC, Tsai TF. Itraconazole in the treatment of nonfungal cutaneous diseases: a review. Dermatol Ther (Heidelb) 2019;9:271–80.

Tsubamoto H, Ueda T, Inoue K, Sakata K, Shibahara H, Sonoda T. Repurposing itraconazole as an anticancer agent. Oncol Lett 2017;14:1240–6.

Turner JA, Johnson PE Jr. Pyrvinium pamoate in the treatment of pinworm infection (enterobiasis) in the home. J Pediatr 1962;60:243–51.

V'lckova-Laskoska MT, Caca-Biljanovska NG, Laskoski DS, Kamberova SJ. Palmoplantar pustulosis treated with itraconazole: a single, active-arm pilot study. Dermatol Ther 2009;22:85–9.

Vuddhakul V, Mai GT, McCormack JG, Seow WK, Thong YH. Suppression of neutrophil and lymphoproliferative responses in vitro by itraconazole but not fluconazole. Int J Immunopharmacol 1990;12:639–45.

Wang E, Xia D, Bai W, Wang Z, Wang Q, Liu L, et al. Hand-foot-skin reaction of grade $\geq$ 2 within sixty days as the optimal clinical marker best help predict survival in sorafenib therapy for HCC. Invest New Drugs 2019;37:401–14.

Yeh CN, Chung WH, Su SC, Chen YY, Cheng CT, Lin YL, et al. Fas. Fas/Fas ligand mediates keratinocyte death in sunitinib-induced hand-foot skin reaction. J Invest Dermatol 2014;134:2768–75.

Yoshida A, Yamamoto K, Ishida T, Omura T, Itoh T, Nishigori C, et al. Sunitinib decreases the expression of KRT6A and SERPINB1 in 3D human epidermal models. Exp Dermatol 2021;30:337–46.

Zhang AY, Camp WL, Elewski BE. Advances in topical and systemic antifungals. Dermatol Clin 2007;25:165–83.